

Volume 26 Number 2 December 1995

ISSN 0046-5828

GEO TECHNICAL

ENGINEERING

Journal of
SOUTHEAST ASIAN GEOTECHNICAL SOCIETY

Sponsored by
ASIAN INSTITUTE OF TECHNOLOGY



GEOTECHNICAL ENGINEERING

CONTENTS

Photographic Feature:

PVD Ground Improvement of Soft Bangkok Clay by Y. TAESIRI and D.T. BERGADO	1
---	---

Main Papers:

Statistical Modelling of Randomly Distributed Fibre-Reinforced Sand by G. RANJAN, R.M. VASAN and H.D. CHARAN	3
Cation Exchange Studies on a Lime Treated Marine Clay by G. RAJASEKARAN and S. NARASIMHA RAO	19
The Simple Pile Load Tests and Its Application by I.M. LEE, M.W. LEE, J.H. LEE and S.W. PAIK	37
Soil Pipe Effects on Pore Pressure Redistribution in Low Permeability Soils by J.J. MCDONNELL and M. TARATOOT	53

Closure Discussion:

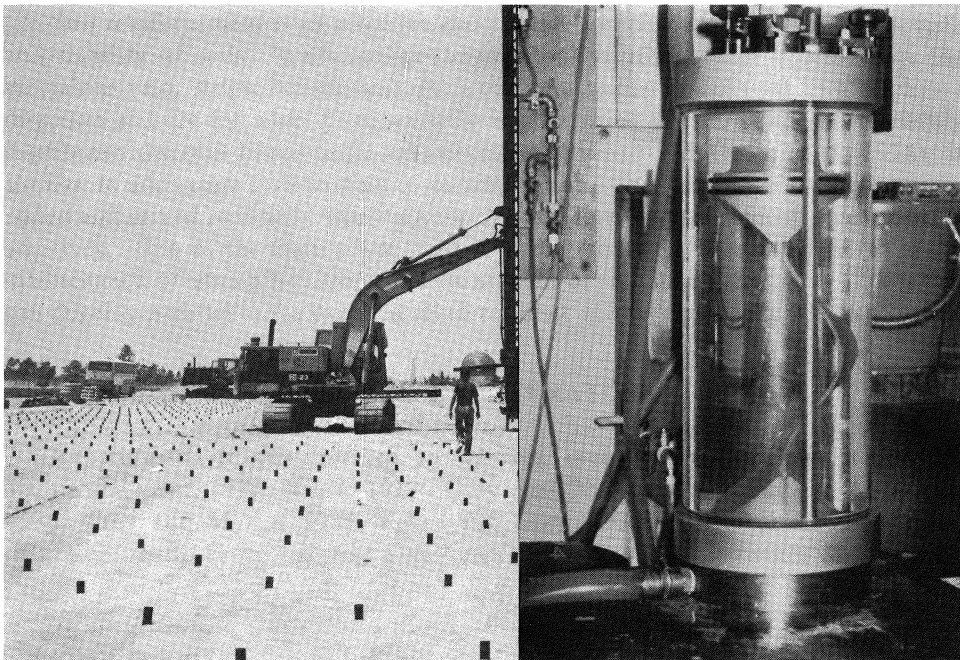
Hyperbolic Method for Evaluation of Settlement of Ground Pretreated by Drains and Surcharge by S.A. TAN	63
Book Review	67
Errata	69
Advertisement	71

PHOTOGRAPHIC FEATURE PVD GROUND IMPROVEMENT OF SOFT BANGKOK CLAY

Y. Taesiri¹, and D.T. Bergado²

The prefabricated vertical drain (PVD) as ground improvement technique of soft clay provides artificial drainage paths and subsequently accelerate the consolidation process. Consequently, the undrained shear strength is increased due to the precompression. The PVD is installed by means of a mandrel which is pushed into the ground by hydraulic or mechanical methods. The PVD is fixed into predetermined position by an anchoring shoe. The quality control testing of PVD to ensure its safe installation includes grab tensile tests, trapezoidal tear test, bursting test and puncture tests. Discharge capacity tests are also done at both straight and deformed conditions to verify the longitudinal drainage of PVD at both straight and deformed conditions. The appropriate ASTM standards can be used for the aforementioned tests.

Currently, PVDs have been used at Second Bangkok Chonburi Highway and the Outer Ring Road Projects of the Thailand Department of Highways. The photograph shows the laboratory PVD testing at deformed condition and the installation of PVD in soft Bangkok clay.



¹ Materials and Research Division, Department of Highways, Sri Ayuthaya Road, Bangkok, Thailand.

² Associate Professor of Geotechnical Engineering, Asian Institute of Technology, GPO Box 2754, Bangkok, Thailand.

STATISTICAL MODELLING OF RANDOMLY DISTRIBUTED FIBRE-REINFORCED SAND

G. Ranjan¹, R.M. Vasan² and H.D. Charan³

SYNOPSIS

A series of triaxial compression tests were carried out on fine sand reinforced with discrete, randomly distributed fibres, both synthetic and natural, to study the influence of fibre parameters (i.e. weight fraction, aspect ratio and modulus), soil-fibre surface friction and confining stress on shear strength of reinforced sand. A regression analysis of test results has been carried out to develop a statistical model to quantify the effect of these factors on the increase in shear strength. The model predicts the relative contribution of each parameter to the strength of reinforced sand. Weight fraction of fibres has been observed to be the most significant parameter for strength increment of sand. The sand fibre composites have a curvilinear failure envelope, with a transition occurring at a certain confining stress, termed as "critical confining stress", below which the fibres tend to slip.

INTRODUCTION

Soil reinforcement is an effective and reliable technique for improving strength and stability of soils. In conventional methods of reinforced-soil construction, the inclusions (e.g. strips, fabrics, bars, grids etc.) are normally oriented in a preferred direction and are introduced sequentially in alternating layers. However, randomly distributed discrete fibre-reinforced soil called 'ply-soil' (McGown et al, 1978), is similar to admixture stabilization in its preparation. The discrete fibres are simply added and mixed randomly with soil, much the same way as cement, lime or other additives. One of the main advantages of using randomly distributed fibres is the maintenance of strength isotropy and the absence of potential planes of weakness that can develop parallel to the oriented reinforcement (Gray and Maher, 1989).

REVIEW OF LITERATURE

Experimental results reported by various investigators (McGown et al, 1978; Verma and Char, 1978; Hoare, 1979; Gray and Ohashi, 1983; Gray and Al-Refeai, 1986; Gray and Maher, 1989; Maher and Gray, 1990; Al-Refeai, 1991) showed that fibre reinforcement causes significant improvement in strength and stiffness

¹ Professor, Dept. of Civil Engineering, Univ. of Roorkee, Roorkee-247667, India.

² Reader, Dept. of Civil Engineering, Univ. of Roorkee, Roorkee-247667, India.

³ Senior Lecturer, Engineering College, Kota-324010, India.

of sand. More importantly it exhibits greater extensibility and small loss of post peak strength (i.e. greater ductility in the composite material) as compared to sand alone or sand reinforced with high modulus inclusions (Gray and Ohashi 1983; Gray and Al-Refeai, 1986). The increase in strength and stiffness is reported to be a function of sand characteristics e.g. particle size, shape and gradation, fibre characteristics e.g. weight fraction, aspect ratio, skin friction and modulus of elasticity and test condition e.g. confining stress (Gray and Maher, 1989; Maher and Gray, 1990, Al-Refeai, 1991). It has been reported that the strength of reinforced sand increases with increase in fibre content, aspect ratio and soil fibre surface friction. A better gradation i.e. increase in coefficient of uniformity, C_u , lower sphericity and smaller average grain size (D_{50}) of sand result in higher fibre contribution to strength (Maher and Gray, 1990).

Hoare (1979) analysing the results of a series of laboratory compression and CBR tests on a sandy gravel reinforced with randomly distributed synthetic fibres < 2% by weight observed that the presence of fibres increased the angle of internal friction and ductility of the soil. Similar observations have been reported by Verma and Char (1978), using triaxial tests on mild steel fibre-reinforced medium/fine sand. They observed an increase in angle of internal friction from 36° to 45° with increase in fibre content from zero to 7% (by volume).

Andersland and Khattak (1979) carried out study on a Kaolinite clay reinforced with paper pulp (cellulose) fibres in triaxial testing under confining stress of 294 kPa to 441 kPa. On the basis of test results, they concluded that the addition of fibres increased both the stiffness and undrained shear strength of the clay. The effective angle of internal friction (ϕ') of reinforced soil was reported to range from 20° for unreinforced clay to 31° for all fibre samples under consolidated drained condition. Also, consolidated undrained tests exhibited the values of ϕ' ranging from 20° for unreinforced clay to 80.4° for samples of fibres only.

Setty and Rao (1987) and Setty and Murthy (1990) carried out triaxial tests, C.B.R. tests and tensile strength tests on silty sand and black cotton soil respectively, reinforced with randomly distributed polypropylene fibres. The test results indicated that both the soils showed significant increase in cohesion intercept and a slight decrease in angle of internal friction (i.e. overall effect is to increase shear strength), with an increase in fibre content of upto 3% (by weight).

Review of Theoretical Development

Literature available on the mechanism of fibre-reinforced soil is limited. A brief review of relevant papers has been presented here. A simple force-equilibrium model was proposed by Waldron (1977) to describe the load-deformation characteristics of soils reinforced with plant roots. He used the original Mohr-Coulomb's equation of shear strength ($s = c + \sigma \tan \phi$) in a modified form, for root-permeated soil as:

$$s_r = c + \sigma \tan \phi + \Delta S \quad (1)$$

where s_r is the shear strength of root-permeated soil and ΔS is the increase in shear strength on account of root reinforcement. The concept of root-reinforcement of soil was utilised by Gray and Ohashi (1983) and, Gray and Al-Refeai (1986) to describe the deformation and failure mechanism of fibre-reinforced soil and to evaluate the increase in shear strength (ΔS) for oriented fibres crossing a shear plane. The model proposed by Gray and Ohashi (1983) consists of a long, elastic fibre extending an equal length on either side of the shear plane. The fibre orientation was considered initially perpendicular to the shear plane or at some arbitrary angle (i). The shearing of soil causes the fibre to distort as shown in Fig.1(b); thereby mobilising tensile resistance in the fibre. The tensile force in the fibre is resolved into the component normal and tangential to the shear plane. The normal component causes an increase in confining stress on the failure plane and the tangential component directly resists shear. The shear strength increase (ΔS) from oriented fibre-reinforcement in sand was estimated by the expressions:

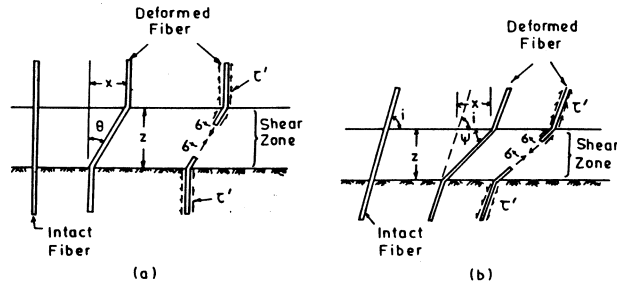


Fig. 1 Model for Oriented Fiber Reinforcement in Sand

$$\text{Perpendicular fibres: } \Delta S = \left[\frac{A_f}{A} \sigma_t \right] (\sin\theta + \cos\theta \tan\phi) \quad (2)$$

$$\text{Inclined fibres: } \Delta S = \left[\frac{A_f}{A} \sigma_t \right] [\sin(90-\psi) + \cos(90-\psi) \tan\phi] \quad (3)$$

$$\psi = \tan^{-1} \left[\frac{1}{\frac{x}{z} + (\tan i)^{-1}} \right] \quad (4)$$

where σ_t = mobilised tensile strength of fibres; $\frac{A_f}{A}$ = fibre area ratio; ϕ = angle of internal friction of sand; θ = angle of shear distortion; i = initial orientation angle of fibre w.r.t. shear surface; z = thickness of shear zone and x = horizontal shear displacement.

Assuming a linear distribution for tensile stress along the length of fibre, Gray and Ohashi (1983) have proposed the following equation for tensile stress in the fibre:

$$\sigma_t = \left[\frac{4E\tau'}{d} \frac{Z}{d} \right]^{1/2} (\sec\theta - 1)^{1/2} \quad (5)$$

where τ' = skin frictional resistance along the fibre, E = modulus of elasticity of fibre and d = diameter of fibre.

The tensile stress developed in the fibre at the shear plane was found to be a function of fibre-properties (i.e. skin friction, length, diameter, weight fraction, modulus etc.) and confining stress.

The shear strength increase (ΔS) and factors affecting it, predicted by force-equilibrium model have been found to be similar to the experimental results obtained from direct shear tests. The maximum shear strength increase, both theoretically and experimentally was observed for fibres placed at an angle of 60° with shear failure plane. Farther, it was mentioned by Gray and Ohashi (1983) that in a direct shear test the orientation of principal tensile strain in a dense sand is approximately of 60° to shear plane. Therefore, fibres should be placed in the direction of principal tensile strain in order to mobilise maximum tensile strain in fibres.

Maher and Gray (1990) proposed a force-equilibrium model with statistical analysis for randomly distributed discrete fibre-reinforced sand. The model predicts the orientation and the quantity of fibres at any arbitrary chosen plane using the statistical theory of composite material (Naaman et. al, 1974). The orientation of the fibres, on average was expected to be perpendicular to the plane of shear failure in triaxial compression tests. The failure plane was assumed to be the same as given by Mohr-Coulomb failure criteria i.e. at an angle of $(45^\circ + \phi/2)$ with horizontal. The average number of fibres, N per unit area crossing the shear plane is given by eq. 6

$$N_f = \frac{2V_f}{\pi d^2} \quad (6)$$

where V_f = volume ratio (volume of fibres per unit volume of soil mass). Also, the fibre area ratio is given by eq. 7

$$\frac{A_f}{A} = N_f \left[\frac{\pi}{4} d^2 \right] \quad (7)$$

where A_f = cross-sectional area of all fibres crossing the shear plane; A = total cross-sectional area of the failure plane, and d = diameter of fibre.

The tensile stress, σ_t developed in the fibre is given by eq.8 (Waldron, 1977),

$$\sigma_t = 2\tau' \frac{1}{d} \quad (8)$$

STATISTICAL MODELLING OF FIBER-REINFORCED SAND

where τ' = skin frictional resistance along the fibre ($= \sigma_{\text{conf.}} \tan \delta$); l = length of the fibre and $\sigma_{\text{conf.}}$ = confining stress.

The shear strength increase, ΔS due to fibre reinforcement was estimated using the force - equilibrium method (eq.2), and expressed as follows:

$$\Delta S = N_f \left[\frac{\pi d^2}{4} \right] \left[2(\sigma_{\text{conf.}} \tan \delta) \frac{1}{d} \right] (\sin \theta + \cos \theta \tan \phi) \quad (\xi) \quad (9)$$

where ξ = an empirical coefficient depending upon sand parameters (i.e. size and shape of sand grains and gradation).

A relatively simple force-equilibrium model (Gray and Ohashi, 1983) proposed for oriented fibres crossing a shear plane, cannot directly be used for randomly distributed fibres. The model proposed by Maher and Gray (1990) has predicted reasonably well the increase in the strength of randomly distributed fibre-reinforced soil. However, the width of shear zone, z which significantly affects the increase in strength (Shewbridge and Sitar, 1989, 1990) has not been determined for reinforced soil. Also, the average expected orientation of fibres was assumed to be perpendicular to the plane of shear failure. However, it is difficult to determine experimentally the orientation of fibres. Thus, in the case of randomly distributed fibre-reinforced soil, the position, the direction and the number of fibres at any plane is quite uncertain.

The main objective of this study is to propose a model based on statistical analysis of triaxial compression tests results and to quantify the effect of fibre properties, sand parameters and confining stress on the increase in shear strength of randomly distributed discrete fibre-reinforced sand.

EXPERIMENTAL PROGRAMME

About 150 triaxial compression tests were performed to determine the effect of confining stress, fibre properties i.e. content, aspect ratio and modulus, degree of compaction and soil-fibre surface friction on the increase in shear strength of fine sand. The tests were conducted using a computer controlled triaxial testing system (GDSTTS) which precisely measures and records the axial stress-strain, radial stress-strain and volume change.

Tests Materials

Reinforcement: Both synthetic and natural fibres were used in the investigation to study the effect of fibre inclusion on the strength of fine sand. Table 1 summarises the properties of the different types of fibres that were used.

Table 1 : Fibre Characteristics

Fibre type	Diameter d(mm)	Specific gravity G_f	Tensile strength (kPa)	Tensile modulus (kPa)	Skin friction angle(δ°)	Aspect ratio (l/d)
Plastic (synthetic)	0.3	0.92	1.5×10^5	3×10^6	21	50,75 100,125
Coir (natural)	0.2	0.75	1.5×10^5	2×10^6	29	50,75 100,125
*Bhabhar (natural)	0.2	0.80	0.75×10^5	1.5×10^6	26	50,75 100,125

* Locally available natural fibre used for making cleaning brush.

Soil: The soil used was a poorly graded fine sand (SP-SM) as per Unified Soil Classification System (USCS). The properties of sand are given in Table 2.

Table 2: Properties of Fine Sand

Effect- ive grain size, D_{10}	Median grain size, D_{50}	Coeffi- cient of unifor- mity, C_u	Specific gravity G_s	Max. void ratio e_{max}	Minimum void ratio e_{min}	$c' - \phi'$ parameters*	
						c' (kPa)	ϕ' (degree)
0.14mm	0.29mm	2.28	2.60	1.08	0.495	10.5	34°

* $c' - \phi'$ parameters were determined by triaxial compression tests on samples prepared at an optimum moisture content (15%) and maximum dry density (16.2 kN/m^3), obtained from standard Proctor's test. Also, since the samples were partially saturated, development of pore pressure, u was observed to be insignificant. Therefore, $(c - \phi) = (c' - \phi')$.

Sample preparation and testing

Fibre-reinforced sand samples were prepared at maximum dry density and optimum moisture content; obtained by conducting standard Proctor tests on unreinforced sand. The amount of fibres to be added to sand was taken as the percentage by weight of soil solids. The amount of fibres and sand required to fill a standard mould of size 38 mm x 76 mm at desired density was taken and water of known quantity (i.e. the optimum moisture content) was added. Fibres were mixed thoroughly by hand to achieve a fairly uniform mix. If fibres are mixed in dry sand, a segregation and/

or floating tendency of fibres was noted. The moist sand-fibre mix was transferred to the mould in three layers and compacted by light tamping of successive layers to achieve a fairly uniform density throughout the depth of the sample. Consolidated undrained triaxial tests were conducted on partially saturated reinforced samples at axial strain rate of 1.25 mm/min. Samples were tested at confining stress of 50-400 kPa applied in single stage, with varying fibre content and aspect ratio.

STATISTICAL MODELLING

The shear strength of fibre-reinforced soil composite depends upon fibre-properties i.e. weight fraction, aspect ratio and modulus of elasticity, soil-fibre surface friction, dry density of soil and confining stress. Modelling of states of stress-strain during deformation and failure in the composite is complex and difficult. Also, since discrete fibres are randomly distributed in a soil mass, their position, direction and the number of fibres crossing a shear plane is quite uncertain. A statistical analysis on triaxial compression tests results has been made to quantify the effect of soil fibre parameters and confining stress on the increase in shear strength of fine sand. The mathematical expression of the model is as follows:

$$\Delta S = f \left[\omega_f, l/d, E_f/E_s, \delta, \sigma_3, \gamma_d/\gamma_{dmax} \right] \quad (10a)$$

where

ΔS = increase in shear strength of fine sand i.e. the difference between major principal stress at failure of fibre-reinforced sand and that of unreinforced sand.

ω_f = weight fraction of fibres (%),

l/d = aspect ratio (length over diameter) of fibre

E_f = modulus of elasticity of fibre

E_s = modulus of elasticity of sand

δ = skin frictional angle,

σ_3 = confining stress.

γ_d = dry density of soil

γ_{dmax} = maximum dry density of sand obtained from standard Proctor's test.

This equation can be written in non-dimensional form, as follows:

$$\frac{\Delta S}{\sigma_3} = f \left(\omega_f, l/d, E_f/E_s, \delta, \gamma_d/\gamma_{dmax} \right) \quad (10b)$$

Before regression analysis of test results can be carried out, it is essential to define the failure condition for fibre-reinforced sand as it does not indicate a peak stress. The stress-strain behaviour of fibre-reinforced sand is very much different

from that of unreinforced sand (Fig.2). Unreinforced sand attains a peak stress at around 10% axial strain which then remains practically constant even up to 20% axial strain, whereas fibre reinforced sand samples do not exhibit any peak stress. The stress-strain curves of reinforced sand indicate an increasing trend even at axial strain of 20%. The failure in such situations is generally defined in terms of serviceability adopting a certain value of permissible amount of deformation. Usually failure stress is taken, corresponding to a strain of 15 or 20 %. Thus, in the present analysis, the failure has been defined as the stress corresponding to the peak stress condition or at 20% axial strain which ever is earlier. Here, shear strength has been defined in terms of major principal stress at failure (σ_{1f}).

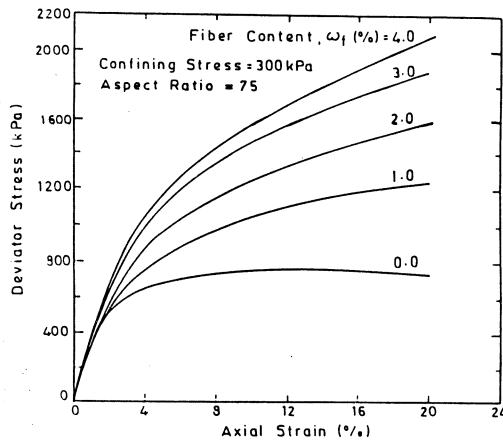


Fig. 2 Stress-Strain Behaviour of Fibre-Reinforced Sand

Regression Analysis

A large number of triaxial test trials of various sand-fibre parameters and confining stress have been used in the regression analysis. The equation of regression for a response function (y) and factors ($x_1, x_2, x_3 \dots$) affecting it can be presented as follows:

$$y_i = a_0 + a_1x_{1i} + a_2x_{2i} + \dots \quad (11a)$$

where $a_0, a_1, a_2 \dots$ are the coefficients and $i = 1, 2, 3 \dots n$, number of trials. This will give n equations.

The difference between the experimental value of y and that obtained from the equation of regression (i.e. residue, U) is given as:

$$y_i - a_0 - a_1x_{1i} - a_2x_{2i} - \dots = U \quad (11b)$$

According to the method of least squares; the residual sum of squares should be a minimum, i.e.

$$\sum_{i=1}^n U^2 = \text{minimum} \quad (11c)$$

A partial derivatives of U with unknown coefficients will provide the required number of simultaneous equations

The simultaneous equations are solved by matrix algebra, as follows:

$$AX = Y \quad (11d)$$

Where A, X and Y are matrices for unknown coefficients, X-values and Y-values respectively. The unknown coefficients can be obtained, as

$$A = X^{-1}Y \quad (11e)$$

The regression analysis used the following assumptions:

- I. The response parameter (ΔS) is a random quantity with a normal distribution law. Most of the distributions in nature follows a law of normal distribution (Adler et al, 1975, Clarke and Cook, 1983; Cooper and Weekes, 1989).
- II. The variance of ΔS does not depend on its absolute value i.e. variances should be homogeneous. The homogeneity of variance and reproducibility of the test are the pre-requisites of regression analysis. The homogeneity of variance has been checked with the Fisher ratio (F-test) and found true at 95% confidence level. Also, each test has been repeated at least twice.
- III. The values of independent factors (i.e. ω_p , l/d , E_p , δ , σ_3 , γ_d) are not random quantities.

The Proposed Model

Combinations of the parameters used in equation (10a) have been studied in the laboratory by conducting triaxial compression tests on fibre-reinforced sand. To evaluate the influence of state of compactness on the strength of reinforced sand, the tests were conducted at different densities (i.e. at 16.2, 15.2 & 14.58 KN/m³). The test results indicate that the difference in gain of strength is of the order of + 2.5-5% with a variation in density from 16.2 KN/m³ to 14.58 KN/m³. This for all practical purposes is insignificant and have therefore been neglected in the modelling.

Fig. 3 shows strength envelopes of fibre reinforced sand. The strength envelopes for reinforced sand are curvilinear with a transition at a certain critical confining stress (σ_{crit}). The increase in strength is attributed to soil fibre surface friction and tensile stress developed in the fibres. The strength increment at low confining stress (σ_3

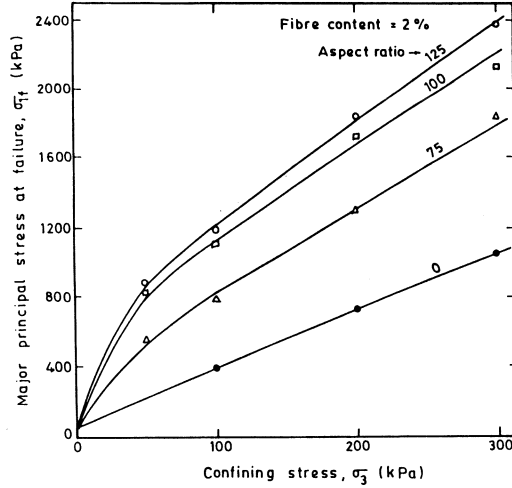


Fig. 3 Principal Stress Envelopes of Fibre-Reinforced Sand

$\leq \sigma_{crit.}$) is because of mobilisation of soil-fibre surface friction and that at high confining stress ($\sigma_3 > \sigma_{crit.}$) is mainly due to the development of tensile stress in the fibres. Thus, the effect of elasticity of fibres (E_f) on the strength increase at low confining stress ($\sigma_3 \leq \sigma_{crit.}$) has been neglected in modelling.

Two mathematical equations have been developed; (i) For $\sigma_3 \leq \sigma_{crit.}$ and (ii) For $\sigma_3 \geq \sigma_{crit.}$.

(i) For $\sigma_3 \leq \sigma_{crit.}$: Various models ranging from polynomial of single degree to higher order have been tested, but the logmodel provided the best fit of the data. The following relationship for increase in strength, ΔS was established:

$$\log_{10} (\Delta S / \sigma_3) = -0.468 + 0.86 \log_{10} (\omega_f) + 0.64 \log_{10} (\delta) + 0.59 \log_{10} (1/d)$$

$$\log_{10} (\Delta S / \sigma_3) = \log_{10} [\text{antilog}(-0.468) \times (\omega_f)^{0.86} \times (\delta)^{0.64} \times (1/d)^{0.59}]$$

$$\Delta S = [0.34 (\omega_f)^{0.86} (\delta)^{0.64} (1/d)^{0.59}] (\sigma_3) \quad (12a)$$

$$R^2 = 0.90, \text{ degree of freedom} = 16$$

where δ is in radians.

(ii) For $\sigma_3 \geq \sigma_{crit.}$: A similar relationship was obtained for $\sigma_3 \geq \sigma_{crit.}$:

$$\Delta S = \left[0.01 (\omega_f)^{0.88} \left[\frac{E_f}{E_s} \times \delta \right]^{0.68} (1/d)^{0.59} \right] (\sigma_3) \quad (12b)$$

$$R^2 = 0.90, \text{ degree of freedom} = 51.$$

where E_s = initial tangent modulus of unreinforced sand

ΔS , $w_f l/d$, E_f , δ , σ_3 are the same as described in equation (10a).

The term R^2 is an index of reliability of the relationship. A regression equation which lies very close to all the observation points will give a high value of R^2 (i.e. $R^2 \approx 1.0$) whereas a scatter of points around the regression equation will give a low value of R^2 . The adequacy of the model (i.e. eqs.12(a) & (b)) and the significance of the coefficients have been checked using the F-test and t-test respectively and found to be true with a 95% confidence level.

The proposed model (eqs. 12(a) & (b) is applicable only for fine sand (average grain size, $D_{50} = 0.29\text{mm}$). To evaluate the effect of sand grain size, D_{50} two more sands, say S2 & S3 (having $D_{50} = 0.45\text{mm}$ & 0.55mm) have been used. All the three soils used are classified as poorly graded sands, having coefficient of uniformity, $C_u = 2.28 - 2.38$. A series of triaxial tests have been carried out on these soils reinforced with plastic fibres of aspect ratio 75 & 100 and weight fraction 0.5 - 2% under confining stress of 50 - 300 kPa. Based on the test results an empirical coefficient (g) has been introduced in the model, as follows:

$$\Delta S = [0.34 (w_f)^{0.88} (\delta)^{0.64} (1/d)^{0.59}] (\sigma_3) (g) \quad (12c)$$

$$\Delta S = \left[0.01 (w_f)^{0.88} \left[-\frac{E_f}{E_s} - x \delta \right]^{0.68} (1/d)^{0.59} \right] (\sigma_3) (g) \quad (12d)$$

For various combinations of fibre aspect ratio, weight fraction and confining stress, the increase in strength, ΔS_2 & ΔS_3 for reinforced sands, S₂ & S₃ respectively have been determined. The ratios of ΔS_2 (or ΔS_3) to ΔS_1 (i.e. strength increase of fine sand) under similar parametric conditions were calculated. Since the value of the empirical coefficient, g equals to one for fine sand, the ratios of strength increase (i.e. $\Delta S_2/\Delta S_1$ or $\Delta S_3/\Delta S_1$) so obtained gives the values of g for the other two sands (i.e. S₂ & S₃). These results have been presented in Fig.4, which can be used to determine the empirical coefficient, g for known value of average sand grain size, D_{50} .

Verification of the Model

No equivalent model is available in the literature, for the verification of the model (eqs.12c & 12d), therefore a new series of triaxial tests were performed on randomly selected soil-fibre parameters. The combination of parameters were selected in such a way that they have not been used in the regression analysis for development of the model. Fig. 5(a) & (b) are comparisons of predicted versus experimental values for the increase in strength for various types of fibres of aspect ratio 75-125 and under confining stress of 50-300 kPa. Most of the points are found to be quite close to 45° - line.

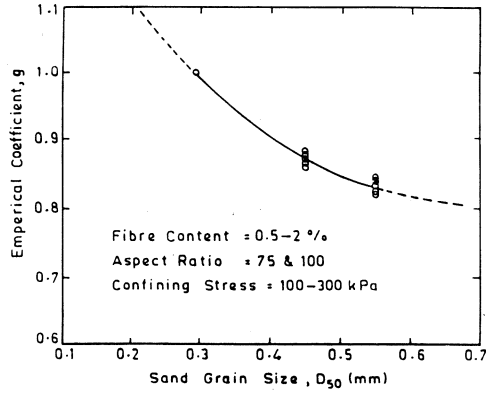


Fig. 4 Empirical Coefficient g versus Average Sand Grain Size

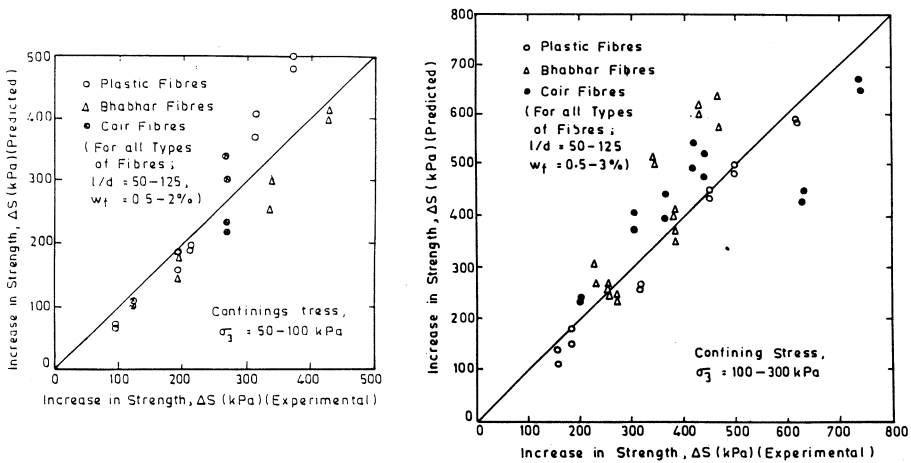


Fig. 5(a) & (b) Verification of Equation 12(c) & (d)

Experimental versus predicted (based on equation 12 (c) & (d)) failure envelopes of reinforced sand for different fibre types and aspect ratio are shown in Fig.6(a),(b) & (c). It is observed that there is a reasonable agreement between the experimental values and those obtained from the model.

CONCLUSIONS

From present experimental investigation and statistical analysis, it is concluded that the increase in strength due to the inclusion of short, randomly distributed fibres is a function of the weight fraction of fibres, aspect ratio, modulus of elasticity, surface friction, sand grain size (other sand parameters being constant) and

STATISTICAL MODELLING OF FIBER-REINFORCED SAND

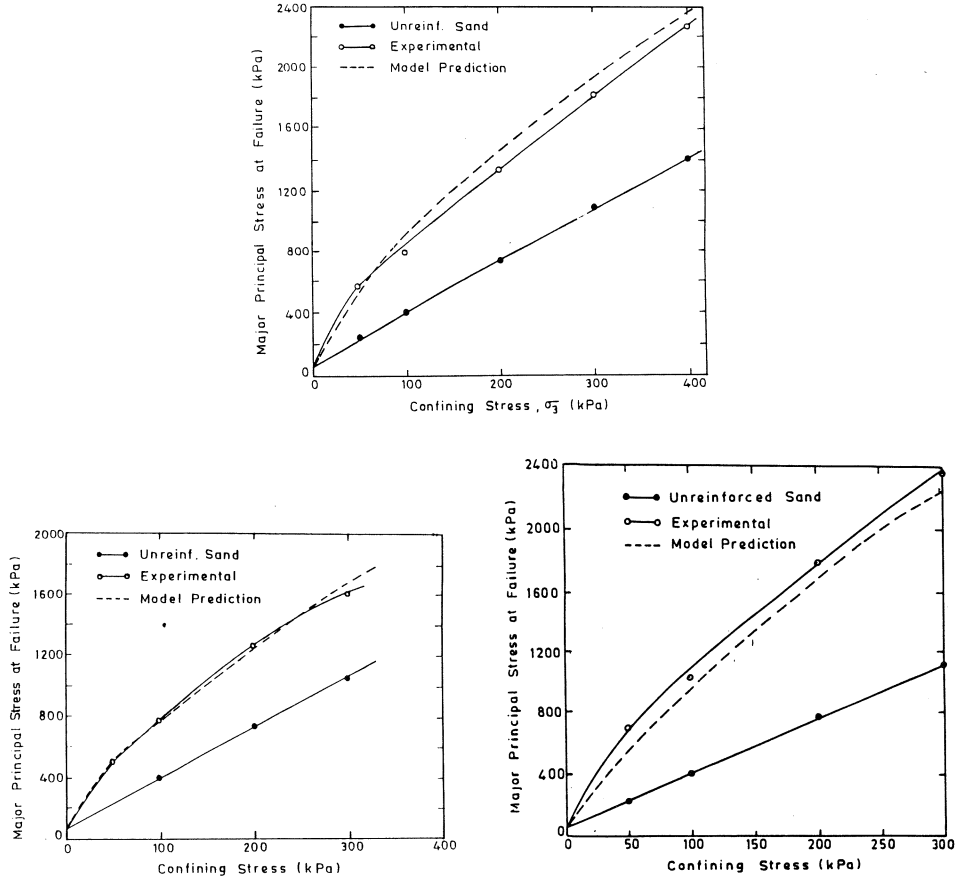


Fig. 6(a), (b) & (c) Experimental versus Predicted Principal Stress Envelope

confining stress. The following conclusions emerged from the present study:

1. The proposed model estimates, reasonably well the increase in strength of sand due to the inclusion of discrete fibres. The relative contribution of each factor to the strength increase may be estimated by the power coefficients of the equation 12(c) & (d). It is clear that the effect of the weight fraction, w_f (having higher value of power coefficient) is the most significant in increasing the strength of sand.
2. The principal stress envelopes for fibre-reinforced sand are bilinear having a transition at a critical confining stress, $\sigma_{crit}^{\#}$ below which the fibres tend to slip or pullout.
3. The inclusion of fibres causes an increase in peak shear strength and reduction in the loss of post-peak stress. Thus, residual strength of fibre-reinforced sand is higher as compared to unreinforced sand.

The proposed model is useful in estimating the likely contribution to shear strength of sand as a result of reinforcement with short, randomly distributed fibres of any type. Further research work is under progress to find the effect of fibre reinforcement on silt/sandy silt and silty sand.

REFERENCES

- ADLER, YU, P. MARKOVA, E.V. and GRANOUSKY, YU. V. (1975) "The Design of Experiments to Find Optimal Conditions" - Mir Publishers Moscow.
- AL-REFEAI, T. (1991) - "Behaviour of Granular Soils Reinforced with Discrete Randomly Oriented Inclusions", - J. Geotextiles and Geomembranes, Vol. 10 (1991), pp.319-333.
- ANDERSLAND, O.B. and KHATTAK, A.S. 1(1979) - "Shear Strength of Kaolinite/Fibre Soil Mixtures" Proc. Int. Conference on Soil Reinforcement, Vol. I, Paris, France, pp 11-16.
- BISHOP, A.W. and HENKEL, D.J. (1969) - "Measurement of Soil Properties in Triaxial Test" - E.L.B.S. - London.
- CLARKE, B.M. and COOKE, D. (1983) - A Basic Course in Statistics" - Edward Arnold Publishers Limited, London.
- COOPER, R.A. and WEEKES, A.J. (1989) - "Data, Models and Statistical Analysis"- Philip Allan Publishers Limited, Oxford (U.K.)
- GRAY, D.H. and AL-REFEAI, T. (1986) - "Behaviour of Fabric versus Fibre-reinforced sand", J. Geotech. Engrg. ASCE 112(8), 804-820.
- GRAY, D.H. and MAHER, M.H. (1989) - Admixture Stabilization of Sand with Discrete, Randomly Distributed Fibres," Proc. XIIth Int. Conf. on SMFE, Rio de Janeiro, Brazil pp 1363-1366.
- GRAY, D.H. and OHASHI, H. (1983) - "Mechanism of Fibre- Reinforcement in Sand," J. Geotech. Engrg. ASCE 109(3) 335-353.
- HOARE, D.J. (1979) - "Laboratory Study of Granular Soils Reinforced with Randomly Oriented Discrete Fibres", Proc. Int. Conf. on use of Fabrics in Geotech, I. Paris, France 47-52.
- MAHER, M.H. and GRAY, D.H. (1990) - "Static Response of sands Reinforced with Randomly Distributed Fibres," - J. Geotech. Engrg. ASCE 116(11) pp 1661-1677.
- McGOWN, A. et al (1978) "Effect of inclusion properties on the Behaviour of Sand," Geotechnique, Vol. 28, No.3, Mar., 1978, pp. 327-346.
- NAMAAN, T., MOAVENZADH, F. and McGARRY, F. (1974) - "Probabilistic Analysis of Fibre Reinforced Concrete" - J. Engineering Mechanics Division, ASCE, Vol. 100, No. EM2, pp397-413.

STATISTICAL MODELLING OF FIBER-REINFORCED SAND

- SETTY, K.R.N.S. and RAO, S.V.G. (1987) - "Characteristics of Fibre reinforced Lateritic Soil" - IGC (87) Bangalore, Vol.1 pp 329-333.
- SETTY, K.R.N.S. and MURTHY, A.T.A. (1990) - "Behaviour of Fibre-reinforced Black Cotton soil," - IGC (1990) Bombay, pp 45-49.
- SETTY, K.R.N.S. and CHANDRASHEKAR, M. (1988) - "Behaviour of Fibre-reinforced Lateritic Soil under Circular Footing" Proc. of First Indian Geotextiles Conference on Reinforced Soil and Geotextiles, Bombay, pp C/41-47.
- SHEWBRIDGE, S.E. and SITAR, N. (1989) - "Deformation Characteristics of Reinforced Sand in Direct Shear", J. Geotech. Engg. Division, ASCE, Vol.115(8), pp.1134-47.
- SHEWBRIDGE, S.E. and SITAR, N. (1990) - "Deformation Based Model for Reinforced Sand", J. Geotech. Engg., Division, ASCE, Vol. 116(7), pp. 1153-1170.
- VERMA, B.P. and CHAR, A.N. (1978) - "Triaxial Tests on Reinforced Sand" - Proc. Symp. Soil Reinforcing and Stabilising Techniques, Sydney.
- WALDRON, L.J. (1977) - "Shear Resistance of Root Permeated Homogeneous and Stratified Soil", Soil Science Society of America, Proceeding Vol. 41, pp 843-

CATION EXCHANGE STUDIES ON A LIME TREATED MARINE CLAY

G.RAJASEKARAN¹ and S.NARASIMHA RAO²

SYNOPSIS

Marine clay deposits of low strength and high compressibility are located in many coastal and offshore areas and, there are several foundation problems associated with these soils. The successful application of lime in stabilizing clayey soils in road and air-field pavements is now being extended to improve the properties of similar soils in-situ either in the form of lime column or lime injection technique. The present investigation deals with an experimental work carried out in the laboratory using lime column and lime injection techniques to stabilize soft clays in marine environment. The lime induced changes occurring in the base exchange of the soil are studied and reported. There is an increase in exchangeable calcium ions concentration in the soil systems from 18 to 35 m.eq/100 g of the soil due to lime treatment. In general, the changes occurring in the other exchangeable cations such as K^+ and Mg^{2+} are not significant. It has been observed that the replacement of sodium ions by calcium ions is quite effective and there is an improvement in the strength of the soil by 8 to 10 times that of the untreated soil. The test results suggest that lime column and lime injection techniques can be conveniently used to improve the behaviour of soft marine clay deposits but one has to be cautious in using lime stabilization technique in soils saturated with sodium sulphate.

INTRODUCTION

Soft marine clay deposits are located in several parts of the world and it is common to find them in coastal regions, continental shelves and offshore areas. Because of their high void ratios, they are characterized by poor strength and high compressibility. The construction of many coastal and offshore structures in these deposits are confronted with many geotechnical problems (BJERRUM, 1973). Treatment of these soils with lime has brought many beneficial effects like improvements in the plasticity characteristics and strength behaviour. A limited application of lime column technique in a modified form was attempted successfully by few researchers for stabilization of soft clays (OKUMARA & TERASHI, 1975 and BROMS & BOMAN, 1975). In these early attempts, the penetration of lime from the columns into the surrounding soil and its induced beneficial effects on cation exchange were not brought out. SOMAYAZULU (1987) used this lime column technique for improving land based clays and confirmed

¹ Research Assistant, Dept. of Civil Engineering, National University of Singapore, Singapore-119260
Former Research Scholar, Ocean Engg. Centre, Indian Institute of Technology, Madras-600 036, India.

² Professor and Head, Ocean Engg. Centre and Dept. of Civil Engg., Indian Institute of Technology, Madras-600 036, India.

the seeping of lime into the surrounding soil. However, there is a necessity to bring out the effectiveness of lime injection technique in marine environment with excessive monovalent (sodium ions) present in the pore water. In the present investigation, an attempt is made to stabilize soft marine clays using both lime columns and lime injection techniques. The influence of the changes in ionic concentration on the efficiency of lime treated clays in marine environment has to be established.

There are many mechanisms put forth to explain the beneficial changes occurring in the lime treated soil systems. One of the mechanism is in the form of base exchange which assumes that divalent calcium cations present in the lime tend to replace the monovalent adsorbed cations present on the soil particle surfaces. It is known that the presence of monovalent cations in the soil pore water system weakens the soil. The efficiency of lime stabilization is known to lie in effective replacement of monovalent cations by calcium ions. In general, the cations are arranged in the order of their replacing power according to the lyotropic series, $\text{Li}^+ < \text{Na}^+ < \text{K}^+ < \text{NH}_4^+ < \text{Rb}^+ < \text{Cs}^+ < \text{Mg}^{2+} < \text{Ca}^{2+} < \text{Sr}^{2+} < \text{Ba}^{2+} < \text{Al}^{3+}$ i.e., any cation tends to replace these to the left of it and monovalent cations are easily replaced by multivalent cations.

Several investigators brought out the effect of cation exchange on soil properties. GRIM (1949) reported that the cation exchange process was partly attributed to the aggregation of soil particles in clays. YONG & WARKENTIN (1966) brought out that due to the replacement of monovalent cations by divalent cations, there was a reduction in the double layer thickness of soil particles. LOKEN (1971) investigated the effect of different cations such as Na^+ , K^+ , Mg^{2+} , Ca^{2+} , Al^{3+} and Fe^{3+} on the plasticity and shear strength properties of a Norwegian clay. The replacing power of these cations mainly depends upon the valency, concentration of ions and charge density of the soil system (SHAINBERG, 1987). Moreover, the zeta potential (interparticle electrical potential difference) was lowered when Ca^{2+} ions replaced lower valency ions and this decreased the number of ions needed to satisfy the required electrical balance.

Limited studies have been carried out to establish the effect of base exchange capacity on the engineering properties of the lime treated soils (KELLEY, 1948 and THOMPSON, 1964). DAVIDSON et al. (1960) one of the first few researchers who suggested that the replacement of monovalent ions such as H^+ and Na^+ by Ca^{2+} induces aggregation effect of soil particles, making the soil more friable and less plastic. The process of calcium cations replacing the monovalent ions by calcium cations present in the oversaturated sodium ion system in sea water has to be confirmed before suggesting lime treatment in submarine soils. Hence in the present investigation, the influence of lime on the base exchange of weak clays in a marine environment has been brought out in the following sections.

An attempt has been made to improve the properties of an Indian marine clay using lime column and lime slurry injection techniques. A testing programme was carried out to establish the changes occurred in the cation exchange properties of different lime treated soil systems. The details of the experimental setups adopted, soil and the chemical additives used are presented in the following sections.

EXPERIMENTAL INVESTIGATIONS

Soil and chemicals used

The soil used was a marine clay procured from the coast of Madras, India (Lat. 13.04°N and Long. 80.17°E) and soil samples were taken at depths of 1 to 2 m. The excavation was carried out by using an open trench excavation method during low tide period. During soil excavation and samples collection, care was taken to pump out the seeping water from the excavated pit. The properties of the untreated soil are given in Table.1.

Table 1. Untreated Soil Properties.

S.No.	Physical and chemical properties	Fresh water system	Sea water system
1.	Liquid Limit	88%	85%
2.	Plastic limit	33%	32%
3.	Plasticity index	55%	53%
4.	pH	7.06	7.3
5.	Organic content	1.36%	1.41%
6.	Sulphates	0.02%	0.20%
7.	Chlorides	0.05%	1.8%
8.	Cation exchange capacity	38 m.eq/100 g of the soil	42 m.eq/100 g of the soil
9.	Lime content	0.91%	0.21%

In the first series of tests, both quicklime (CaO = 95%) and hydrated lime (Ca(OH)₂ = 90%) were used as column filling materials. The effectiveness of lime in a marine environment has to be critically looked into and hence, there is a necessity to bring out the utility aspect of lime along with compounds usually present in sea bed soils. To consider this aspect, in a few test setups, lime with calcium sulphate (96%), sodium sulphate (99%) and calcium chloride (98%) additives were used in the columns. In the second setup, hydrated lime slurry injection under pressure was attempted in a larger test tank.

Test programme

Basically, there were two experimental setups used in this investigation. In the first

setup, lime column work was carried out in a circular tank of diameter 600 mm and 550 mm height (Fig.1). A homogeneous soil bed was prepared to the required thickness of 500 mm and, lime columns of 50 mm diameter and 500 mm height were installed at the centre of the soil bed. Having established that lime diffused into the soil in significant quantities, in the second setup, the testing was further extended using a lime injection technique. This test was carried out in a tank of size, 1000 mm x 1000 mm x 750 mm filled with a soft marine clay (Fig.2). The lime injection was carried out in three stages. First, a steel injection pipe of inner diameter 18 mm and of length 1250 mm was slowly pushed into the soil strata until it reached the bottom of the soil bed. The pipe had 40 perforations over a length of 300 to 400 mm in the bottom portion. Lime slurry with 40% concentration (by weight) was forced through the pipe into the soil bed under a pressure range of 0.2 to 0.3 N/mm². Then, the pipe was slowly withdrawn in stages and the slurry was injected to the middle and top layers of 200 mm height in two stages.

In most of the series, sea water was used for mixing with soil to maintain the required consistency but in one setup, the soil bed was formed under fresh water conditions to bring out the variation in exchangeable sodium ions present. Free water of 50 mm was always maintained on the top of the soil bed. To avoid free swelling of the soil, a nominal surcharge pressure of 5 kN/m² was applied vertically using a

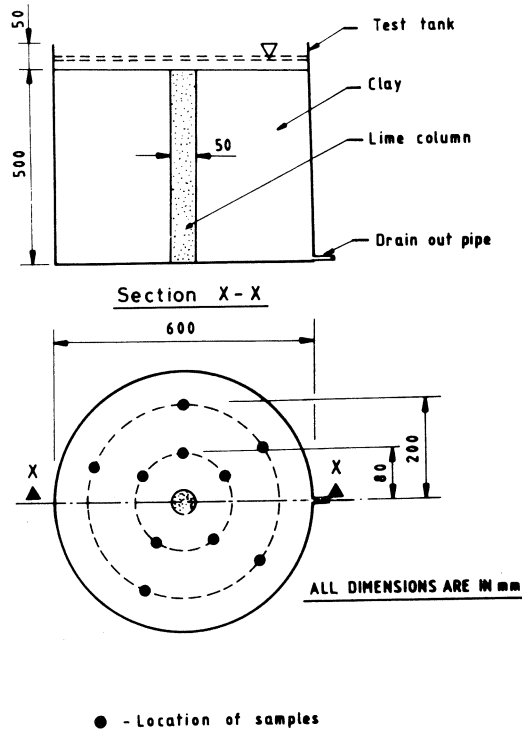


Fig. 1 Details of Experimental Setup for Lime Column Work.

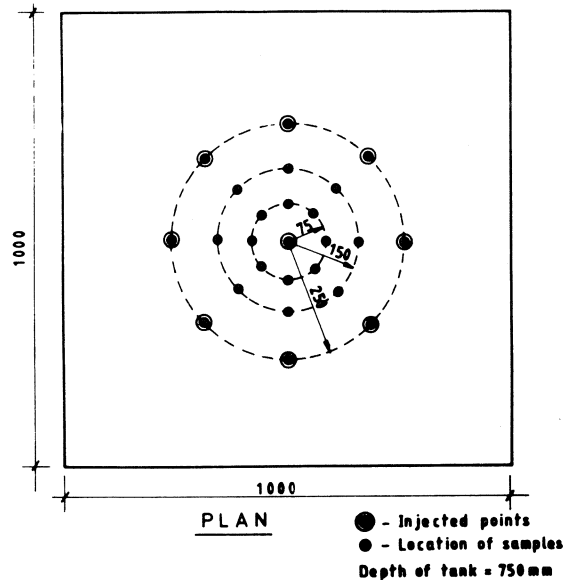


Fig. 2 Details of Experimental Setup for Lime Injection Work.

hydraulic jack and perforated plate arrangement for all the test setups before the lime treatment work was taken up. To establish the effect of lime stabilization on the various properties of the marine clay, a number of representative soil samples were collected from the various experimental setups. These samples were collected at different depths and at various time periods of 2, 7, 15, 30 and 45 days. In lime injection treated soil system samples were taken up to 120 days. The various test procedures adopted are explained in the following sections.

RESULTS AND DISCUSSIONS

Variation in exchangeable cations

It is necessary to know the types of cations present in the soil system for establishing the complete system chemistry of the pore water-electrolyte system. The cations present in untreated and treated soil systems were estimated using an atomic absorption spectrophotometer as per the procedure given by JACKSON (1958) and the values are given in Table. 2. 50 g of air-dried powdered samples were treated with 500ml of 1N ammonium acetate (NH_4OAc) and allowed to stand overnight. The sample was then filtered using Whatman No.42 filter paper and the collected filtrate was analysed to estimate the exchangeable cations viz., sodium (Na^+), Potassium (K^+), calcium (Ca^{2+}) and magnesium (Mg^{2+}) present in different lime treated soil systems.

Table 2. Exchangeable Cations Present in the Untreated Soil Systems

S.No.	Cations present	Test values (m.eq/100 g of soil)	
		Soil in fresh water setup	Soil in sea water setup
1.	Na ⁺	3.8	5.6
2.	K ⁺	2.9	3.3
3.	Ca ²⁺	18.6	19.2
4.	Mg ²⁺	12.8	13.6

The results obtained from samples taken around the quicklime column installed in soil with fresh water are presented in Fig.3. It indicates that the Ca²⁺ ions concentration is increased from 18.6 to 33 m.eq/100 g of the soil whereas the K⁺ ions concentration is increased from 2.9 to 4.6 m.eq/100 g of the soil. A marginal decrease in sodium ions from 3.8 to 1.3 m.eq/100 g of the soil and magnesium ions from 12.8 to 11 m.eq/100 g of the soil after 45 days of treatment are also observed. The increase in Ca²⁺ ions indicates that a significant amount of lime is diffused up to a radial distance of 4 to 6 times the diameter of the lime column from the centre column to the surrounding soil. There is a marginal reduction in the sodium ions concentration but the changes occurred in the K⁺ and Mg²⁺ ions are not significant.

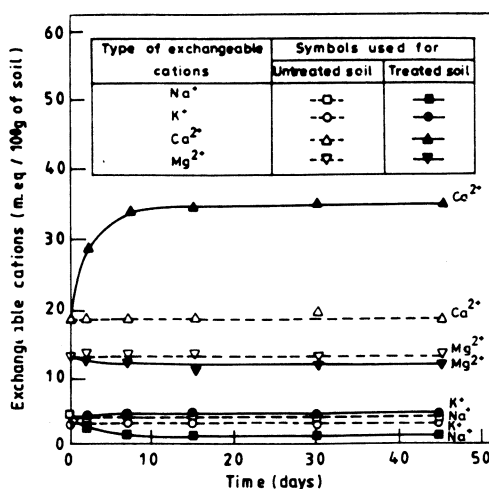


Fig. 3 Variation in Exchangeable Cations with Time for Quicklime Column Treated Soil System in Fresh Water Setup.

CATION EXCHANGE STUDIES ON A LIME TREATED CLAY

For quicklime column setup with sea water, there is an increase in Ca^{2+} ions from 19.2 to 33.9 m.eq/100 g of the soil (Fig.4). There is an increase in K^+ ions concentration from 3.3 to 4.6 m.eq/100 g of the soil and a decrease in Na^+ ions concentration from 5.6 to 1.3 m.eq/100 g of the soil. Disappearance of Na^+ ions in the adsorbed complex in sea water system is quite remarkable and this encourages the use of lime column type of technique in submarine soils. Also, there is a decrease in Mg^{2+} ions from 13.6 to 12.4 m.eq/100 g of the soil. Figs.3 and 4 show that there is an increase in the concentration of Ca^{2+} ions with time. The changes that occurred in the K^+ and Mg^{2+} ions are not significant and there is not much variation of exchangeable cations concentration for both fresh water and sea water treated quicklime column soil systems.

Fig.5 indicates the variation of cations in the hydrated lime column treated soil system in sea water setup. There is an increase in the Ca^{2+} ions from 19.2 to 30.7 m.eq/100 g of the soil and K^+ ions from 3.3 to 4.6 m.eq/100 g of the soil. There is a decrease in other ions such as Mg^{2+} and Na^+ ions from 13.6 to 12.4 m.eq/100 g of the soil and 5.6 to 2.6 m.eq/100 g of the soil respectively. In this system, the increase in the Ca^{2+} ions concentration is slightly lower in comparison with quicklime column treated soil systems. This may be partly due to less hydration effect of lime in this system; whereas in quicklime column systems, the hydration effect is quite significant. The variation of cations in the quicklime-sand column treated soil system shows an increase in the Ca^{2+} ions from 19.2 to 33.3 m.eq/100 g of the soil (Fig.6). There is a decrease in the cations Na^+ and Mg^{2+} from 5.6 to 1.3 m.eq/100 g of the soil and 13.6 to 11.1 m.eq/100 g of the soil respectively. The lime induced changes on other cations are more or less the same as observed in other lime treated soil systems.

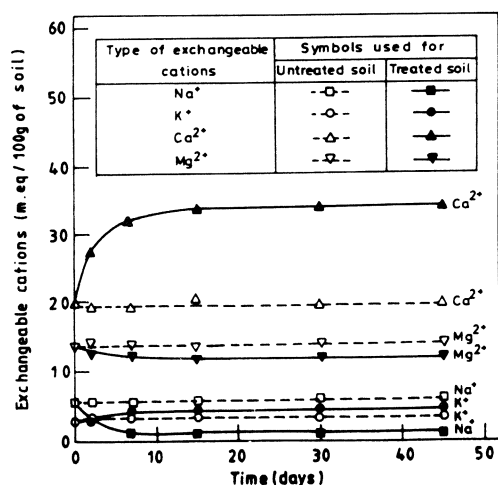


Fig. 4 Variation in Exchangeable Cations with Time for Quicklime Column Treated Soil System in Sea Water Setup.

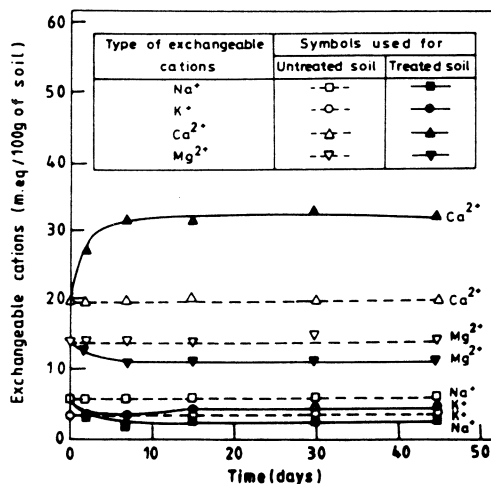


Fig. 5 Variation in Exchangeable Cations with Time for Hydrated lime Column Treated Soil System in Sea Water Setup.

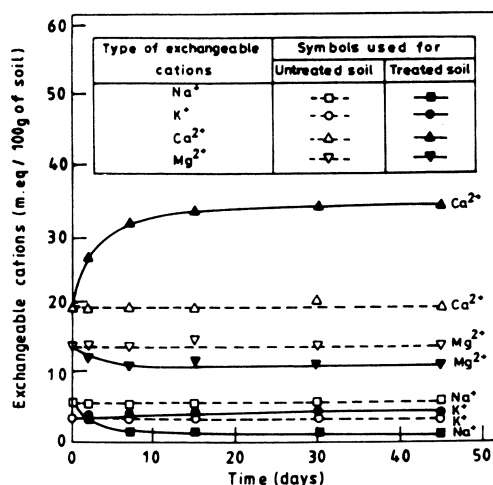


Fig. 6 Variation in Exchangeable Cations with Time for Quicklime-Sand Column Treated Soil System in Sea Water Setup.

In the quicklime-calcium chloride treated soil system, there is an increase in the Ca²⁺ ions from 18 to 37.2 m.eq/100 g of the soil (Fig.7). The other cations such as Na⁺ and K⁺ show a decreasing trend (from 5.6 to 0.98 m.eq/100 g of the soil) and increasing trend (from 3.3 to 5.22 m.eq/100 g of the soil) respectively. There is a decrease in Mg²⁺ ions from 13.6 to 10 m.eq/100 g of the soil. The addition of calcium sulphate with quicklime also shows an effective increase in the Ca²⁺ ions concentration from 19.2

CATION EXCHANGE STUDIES ON A LIME TREATED CLAY

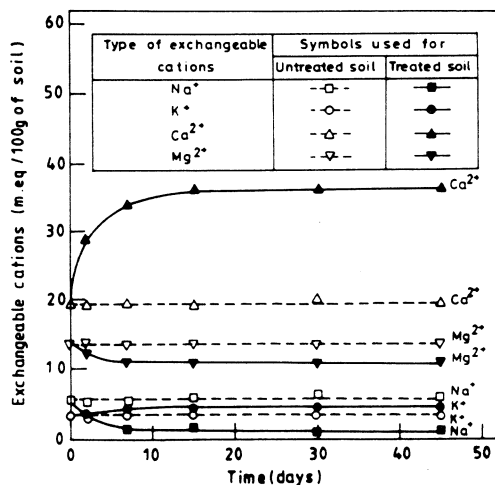


Fig. 7 Variation in Exchangeable Cations with Time for Quicklime-Calcium Chloride Column Treated Soil System in Sea Water Setup.

to 35.9 m.eq/100 g of the soil (Fig.8). There is not much variation in the cations concentration after a time period of 10 to 15 days treatment. The variation in K⁺ ions is negligible (from 3.3 to 4.9 m.eq/100 g of the soil). There is a reduction in Na⁺ and Mg²⁺ ions from 5.6 to 0.98 m.eq/100 g of the soil and 12.8 to 10.4 m.eq/100 g of the soil respectively. The test results show that the addition of admixtures such as calcium chloride and calcium sulphate with lime brings out better changes in the cation concentration and the exchange process is slightly faster.

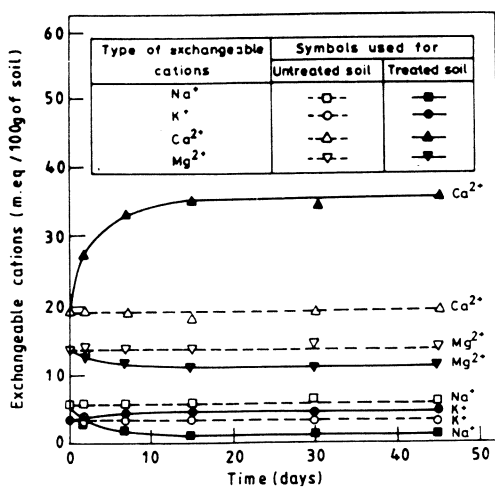


Fig. 8 Variation in Exchangeable Cations with Time for Quicklime-Calcium Sulphate Column Treated Soil System in Sea Water Setup.

In quicklime-sodium sulphate column treated soil system in sea water setup, there is an increase in the Ca^{2+} ions from 19.2 to 26.1 m.eq/100 g of the soil (Fig.9). The increase in these ions is 2 times less than as observed in other systems. This indicates that the presence of sodium sulphate affects the increase of Ca^{2+} ions. A decrease in the Mg^{2+} ions concentrations from an initial value of 13.6 to 11.1 m.eq/100 g of the soil is observed. Also, there is a marginal increase in the K^+ ions concentration from 3.3 to 5.22 m.eq/100 g of the soil. At the same time, it has been observed that there is an increase in the Na^+ ion concentration from 5.6 to 9.8 m.eq/100 g. of the soil. This decrease in the concentration of Ca^{2+} ions is due to the domination of Na^+ ions supplied from the sodium sulphate additive to the soil.

The lime injection soil system (with injection points at a radial distance of 250 mm from the central injected point) shows the same trend of variation of cations as that of the quicklime column in sea water treated soil system (Fig.10). There is an increase in the Ca^{2+} ions from 19.2 to 32.6 m.eq/100 g of the soil within a time period of 7 to 10 days. There is not much variation in the other cations concentration such as Na^+ , K^+ and Mg^{2+} . The test results indicate that there are not much differences in the cations concentration for different lime treated soil systems. The variation in cations concentration due to lime treatment after 15 to 20 days is not significant.

In general, for all lime treated soil systems (Figs.3 to 10), an increase of Ca^{2+} ions concentration from 19.2 to 30-33 m.eq/100 g of soil is seen. Practically there is no change in K^+ ions. Also, there is an overall reduction of Na^+ ions from 5 to 1 m.eq/100 g. of soil except quicklime-sodium sulphate column treated soil system, whereas Mg^{2+} ions concentration is reduced from 13.6 to 11 m.eq/100 g of soil. All these exchange reactions are completed within an initial time period of 7 to 10 days treatment.

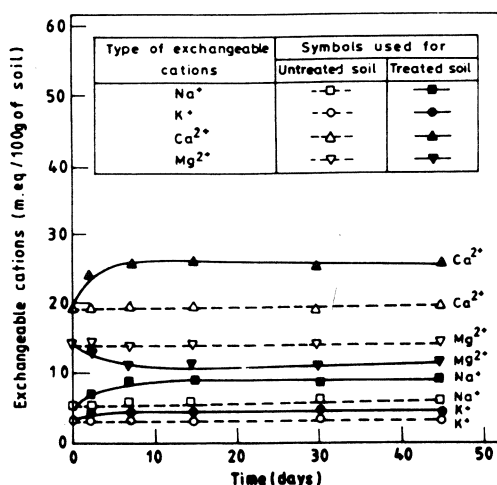


Fig. 9 Variation in Exchangeable Cations with Time for Quicklime-Sodium Sulphate Column Treated Soil System in Sea Water Setup.

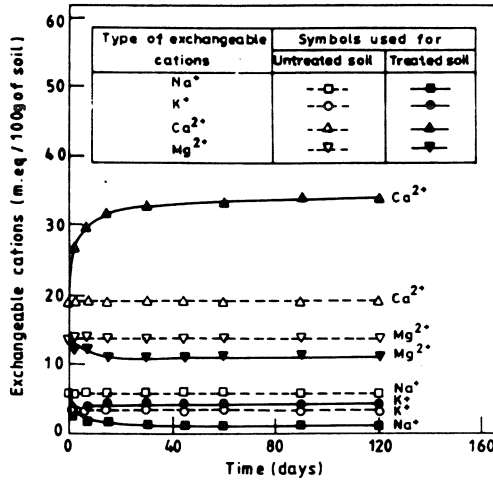


Fig. 10 Variation in Exchangeable Cations with Time for Lime Injection Treated Soil System in Sea Water Setup.

Due to the diffusion of lime into the soil, there is an increase in the alkalinity of the soil system and more cations are adsorbed by the soil particles because of the increased dissociation of weakly acidic SiOH groups exposed on clay crystal edges as reported by earlier investigators (SCHOFIELD, 1949 and HO and HANDY, 1963). The increased adsorption of Ca²⁺ ions to the clay surfaces at high pH causes the clay particles to bind together and results in the improved engineering behaviour of the soil. The cation with the smallest hydrated radius (such as Ca²⁺ ions) moves closest to the micellar surface and is more strongly adsorbed by the soil particles according to the law of mass action (YONG & WARKENTIN, 1966). The measured exchangeable cations concentration for different lime treated soil systems show that the base exchange capacity is more for the soil systems treated with quicklime and inorganic additives such as calcium sulphate and calcium chloride. No significant changes occurred in the exchangeable Ca²⁺ ions concentration for all test setups.

Variation in strength

It has been confirmed that the reaction of the lime with the clay soil results in the strength improvement of the soil and this aspect has been confirmed by many investigators (INGLES, 1964; BALASUBRAMANIAM et al., 1989 and RAJASEKARAN, 1994). To confirm this aspect, strength tests have been conducted in all lime treated soil systems and the variation in strength with time was investigated using an in-situ cone penetrometer specially made for this purpose (Table 3). The procedure followed was in accordance with ASTM D 3441-86 (1989). These results indicate that the strength has been improved by 5 to 8 times that of untreated soil after 45 days treatment. In comparison to the other lime treated soil systems, it can be stated

Table 3. Variation in Strength with Time for Different Lime Treated Soil Systems*.

Sl.No.	Types of treatment	Radial distance of the samples = 80 mm						Radial distance of the samples = 200 mm									
		Time (days)						Time (days)									
		2	7	15	30	45	60	90	120	2	7	15	30	45	60	90	120
1.	Quicklime column treated soil system in fresh water setup																
	Top	1.8	4.1	7.4	9.8	10.2				1.1	2.5	5.1	6.9	8.1			
	Middle	1.75	3.1	5.2	7.8	8.3				1.5	2.2	4.3	6.7	7.2			
	Bottom	1.9	3.7	6.6	9.2	10.1				1.3	2.8	5.8	7.5	8.2			
2.	Quicklime column treated soil system in sea water setup																
	Top	2.1	4.5	6.6	8.4	9.1				1.3	3.8	5.8	7.4	8.3			
	Middle	1.8	3.9	5.4	7.4	8.2				1.8	4.2	5.1	6.6	7.3			
	Bottom	2.1	4.2	6.3	8.4	9.1				1.2	3.4	5.2	7.1	8.1			
3.	Quicklime column treated soil system in sea water setup (120 days test)																
	Top	1.2	2.8	4.1	5.8	6.7	8.6	9.3	9.3	1.1	2.4	3.1	4.4	5.3	6.7	7.2	7.8
	Middle	1.1	1.8	3.5	4.8	6.2	7.9	8.8	9.3	1.1	1.8	2.7	3.9	4.7	6.1	7.1	7.1
	Bottom	1.40	2.3	3.8	4.7	6.1	7.4	8.8	9.1	1.1	1.7	2.7	3.4	4.5	7.2	8.1	8.4
4.	Hydrated lime column treated soil system in sea water setup																
	Top	2.6	3.8	4.7	5.8	6.3				2.1	2.6	3.5	3.7	5.1			
	Middle	1.4	2.7	3.8	4.3	5.4				1.4	2.5	3.1	4.1	4.9			
	Bottom	1.8	3.6	4.7	5.2	6.1				1.7	2.2	4.1	4.7	5.3			
5.	Quicklime-Sand column treated system in sea water setup																
	Top	2.3	3.8	4.7	6.2	6.8				1.8	3.2	3.9	6.1	6.2			
	Middle	1.3	2.4	5.2	6.8	7.1				1.1	1.8	4.2	5.1	5.9			
	Bottom	2.1	3.2	4.6	6.1	6.8				1.4	2.3	3.2	5.0	6.5			

* Strength values are measured using insitu-cone penetrometer ($\tau_{\text{treated}} / \tau_{\text{untreated}}$)

Table 3. (Cont.)

S.No.	Types of treatment	Radial distance of the samples = 80 mm						Radial distance of the samples = 200 mm										
		Time (days)						Time (days)										
		2	7	15	30	45	60	90	120	2	7	15	30	45	60	90	120	
6.	Quicklime-Calcium chloride column treated soil system in sea water setup	Top	2.9	6.1	10.1	11.2	11.2			1.4	3.2	7.2	9.1	9.7				
		Middle	2.7	6.1	10.1	11.1	11.6			1.1	2.2	6.3	8.1	8.9				
		Bottom	1.9	5.4	9.6	10.8	11.1			1.9	4.4	7.1	9.8	10.2				
7.	Quicklime-Calcium sulphate column treated soil system in sea water setup	Top	3.1	4.9	5.1	9.3	9.8			2.1	4.1	6.2	8.8	9.0				
		Middle	2.2	4.3	7.9	10.1	10.8			1.7	3.4	6.5	8.6	9.2				
		Bottom	2.8	4.5	7.8	10.2	10.4			1.9	3.8	6.6	8.9	8.9				
8.	Quicklime-Sodium sulphate column treated soil system in sea water setup	Top	1.1	2.1	2.9	2.1	1.9			1.1	1.2	1.7	1.8	1.9				
		Middle	1.1	1.2	2.2	2.2	1.2			1.7	2.1	2.1	2.1	1.9				
		Bottom	1.90	2.8	3.7	4.3	3.9			1.4	2.0	2.3	3.2	2.7				
9.	Hydrated lime injection treated soil system in sea water setup	Top	1.8	2.60	4.1	6.3	8.2	9.9	10.2	10.2	1.2	1.9	3.3	5.7	7.3	8.2	9.3	9.8
		Middle	1.2	2.2	3.6	7.4	8.9	9.2	9.5	9.7	1.1	1.4	2.9	6.1	7.8	8.9	9.6	9.7
		Bottom	1.9	2.7	4.1	6.5	8.1	9.8	9.8	10.2	1.2	2.4	3.3	6.1	7.8	8.9	10.1	10.3

that the lime in the presence of sodium sulphate is not very effective in improving the soil behaviour. The increase in Na^+ ions concentration with time brings down the efficiency of the lime treatment.

Variation in conductivity

It has been established by earlier investigators that the diffusion/addition of chemicals into the soil induce several changes in the pore fluid system chemistry and affects the ionic concentration of the soil. The variation in this ionic concentration with time can be conveniently measured by using a Conductivity Meter. It is known that the conductivity of the soil-lime mixtures increases with the increase in lime concentration (BHASIN et al. 1988). On this basis, a series of tests were conducted on different lime treated soil samples to investigate the variation of conductivity with time. The procedure adopted was in accordance with the specifications given by JACKSON (1958).

Samples were collected from all test tanks at a radial distance of 100 mm away from the column/injection points at different time periods. The variation in conductivity of different lime treated systems with time is shown in Fig. 11. There is a significant increase in the conductivity of the quicklime treated soil in fresh water setup from 2.92×10^{-3} SYMBOL 87 \f “Symbol” to 4.64×10^{-3} SYMBOL 87 \f “Symbol” after 45 days treatment. For the quicklime column setup in sea water, the increase in

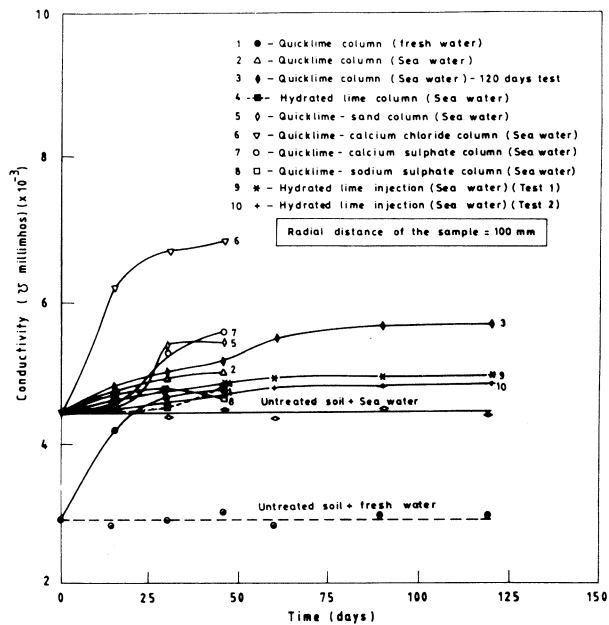


Fig. 11 Variation in Conductivity of Different Lime Treated Soil Systems with Time.

CATION EXCHANGE STUDIES ON A LIME TREATED CLAY

conductivity is only from 4.46×10^{-3} SYMBOL 87 \f “Symbol” to 4.9×10^{-3} SYMBOL 87 \f “Symbol” and with time, this has been improved to 5.7×10^{-3} SYMBOL 87 \f “Symbol”. The improved values of conductivity in the sea water system are due to the salts present in the system. In the case of system with hydrated lime column setup, the marked changes in conductivity could not be observed. The hydrated lime column treated system shows only a marginal increase from 4.46×10^{-3} SYMBOL 87 \f “Symbol” to 4.63×10^{-3} SYMBOL 87 \f “Symbol”. The quicklime-sand column treated system shows an improvement of conductivity up to 4.9×10^{-2} SYMBOL 87 \f “Symbol”. But the addition of additives like calcium sulphate with quicklime increases the conductivity to 5.5×10^{-3} SYMBOL 87 \f “Symbol” and at the same time, the quicklime-calcium chloride mixture increases the conductivity to a maximum value of 6.8×10^{-3} SYMBOL 87 \f “Symbol” after 45 days treatment.

In the case of quicklime-sodium sulphate column treated system, the conductivity increases to a value of 4.76×10^{-3} SYMBOL 87 \f “Symbol” in a time period of 25 days and later, it decreases to 4.61×10^{-3} SYMBOL 87 \f “Symbol”. The initial increase is mainly due to the dominant influence of Ca^{2+} ions but later, the migration of Na^{2+} ions retards the penetration of Ca^{2+} ions and decreases the conductivity of the soil system. The lime injection treated soil system has shows an increase in concentration of the soil system up to a maximum value of 4.63×10^{-3} SYMBOL 87 \f “Symbol” to 4.74×10^{-3} SYMBOL 87 \f “Symbol”. All the test results indicate that there is an overall increase in the conductivity of the soil system with time except in the quicklime-sodium sulphate column treated soil system. The maximum increase in trend is observed up to a time period of 15 to 30 days. The test results indicate that there is an overall increase in the ionic concentration of the soil system and this is mainly due to the diffusion of various ions from the column/injection point. The diffusion of lime into the soil system alters the particulate system and further an increase in the strength behaviour has been noticed as reported in the earlier section. All these factors combine together to improve the soil behaviour with time.

CONCLUSIONS

The following main conclusions were obtained from the above experimental programme. For most of the systems attempted, there is an appreciable improvement in the Ca^{2+} cations and it is quite encouraging to note that there is a reduction in the sodium (Na^+) ions with time. There is an increase in Ca^{2+} ions concentration in all treated systems (varies from 19.2 m.eq/100 g of the soil to 35 m.eq/100 g of the soil) with a corresponding decrease in the sodium Na^+ ions concentration (from 5.6 m.eq/100 g of the soil to 1 m.eq/100 g of the soil). Even in the presence of salt water, there is no decrease in the Ca^{2+} cations adsorbed. It is suggested that the penetration of lime has resulted in improved cationic concentration of soil system and induced several changes in the particulate system. Almost complete replacement of Na^+ cations can be seen in all the systems except the quicklime-sodium sulphate column treated soil system. The

results of this investigation have established that the presence of excessive sodium ions in sea water do not retard the effective penetration of lime into the soil. Thus, both the lime column and lime injection techniques can be conveniently used to improve the behaviour of soft marine clay deposits.

REFERENCES

- ASTM D 3441-86. (1989). Standard test method for deep quasi-static, cone and friction-cone penetration tests of soils, Annual Book of ASTM Standards, Vol.04.08, pp.414-419.
- BHASIN, N.K., DHAWAN, P.K. & MEHTA, H.S. (1988). Lime requirement in soil stabilization, Highways Research Record Bull. No.36, New Delhi, India.
- BALASUBRAMANIAM, A.S., BERGADO, D.T., BUENSUCESO Jr, B.R. & YANG, W.C. (1989). Strength and deformation characteristics of lime treated soft clays, J. of Geotech. Engg., Vol.20, pp.49-65.
- BJERRUM, L. (1973). Geotechnical problems involved in foundation of structures in North Sea, Geotechnique, Vol.23, pp.319-358.
- BROMS, B. & BOMAN, P. (1975). Lime stabilized columns, 5th Asian Reg. Conf. on SM and FE, Bangalore, India, Vol.1, pp.227- 234.
- DAVIDSON, D.F., METEOS, M. & BARNES, H.F. (1960). Improvement of lime stabilization of montmorillonitic clay soils with chemical additives, Highway Research Board Bull. No.262, Washington, D.C., pp.33-50.
- GRIM, R.E. (1949). The composition on relation to the properties of certain soils, Geotechnique, Vol.1, pp.139-147.
- HO, C. & HANDY, R.L. (1963). Characteristic of lime retention by montmorillonite clays, Highway Research Record Bull. No.29, Washington, D.C., pp.55-69.
- INGLES, O.G. (1964). The nature and strength of interparticle bonds in natural and stabilised soil, D3-9, Proc. of a Colloquium on Mech. of soil stabilization, Sydnal, Victoria, Australia.
- JACKSON, M.L. (1958). Soil chemical analysis, Prentice-Hall Int. Inc., London.
- KELLEY, W.P. (1948). Cation exchange in soils, Rheinhold, Publication Co., New York.
- LOKEN, T. (1971). Recent research at the Norwegian Geotechnical concerning the influence of chemical addition on quick clay, Norwegian Geotech. Inst. Pub. No.87., Oslo.
- OKUMARA, T. & TERASHI, M. (1975). Deep lime mixing method of stabilization for marine clay, 5th Asian Reg. Conf. on SM and FE, Bangalore, Vol.1, pp.69-75.

CATION EXCHANGE STUDIES ON A LIME TREATED CLAY

- RAJASEKARAN, G. (1994). Physico-chemical behaviour of lime treated marine clay, Ph.D Thesis, I.I.T, Madras, India..
- SCHOFIELD, R.K. (1949). Effect of pH of electric charges carried by clay particles, J. of Soil Science, Vol.1, pp.1-8.
- SHAINBERG, I. (1987). The effect of exchangeable sodium and electrolyte concentration on crust formation, Advances in Soil Science, Vol.1, pp.101-102.
- SOMAYAZULU, J.R. (1987). Experimental studies of lime columns in soils, Ph.D Thesis, Indian Institute of Technology, Madras, India.
- THOMPSON, M.R. (1964). The significance of soil properties in lime-soil stabilization, Highway Engineering Series No.13, Illinois Co-Op Highway Research Programme, Illinois.
- YONG, R.N. & WARKENTIN, B.P. (1966). Introduction to soil behaviour, The Macmillan Co., New York, p.451.

THE SIMPLE PILE LOAD TEST and ITS APPLICATIONS

I.M. Lee¹, M.W. Lee², J.H. Lee³ and S.W. Paik⁴

SYNOPSIS

Since pile load tests are a time and money consuming process, as an alternative, the Simple Pile Load Test (SPLT) was developed. In spite of its simplicity, the new technique has some shortcomings to be evaluated for practical use. Two major concerns in this paper are the effect of load direction on shaft resistance and the effect of pile tip size on end bearing capacity. In order to examine these points, the laboratory tests using calibration chamber were performed. As a result, the new technique tends to underestimate the shaft resistance, and provides somewhat larger values of end bearing capacity in the uniform sand layer, but provides slightly smaller values of end bearing capacity in weathered granite overlaid by sand. In order to propose the new design correlations based on the standard penetration number, SPLTs were applied in three sites and correlations between the standard penetration number and the bearing capacity are made.

INTRODUCTION

Although many theoretical and empirical approaches to predict pile bearing capacity have been developed so far, no method among them can be applied with certainty. Recent advances in soil mechanics and foundation engineering give useful information about various factors such as concepts of critical depth, mode of deformation and parameters of cavity expansion theory which affect the pile bearing capacity ; however, consideration of all the factors in analyses is nearly impossible and thus some assumptions can not be avoided in the most theoretical approaches. Therefore, the estimated pile bearing capacity based on the results of various methods should be confirmed by field pile load tests. Unfortunately, field tests have been restricted by time and expenses that are major concerns in construction work. To improve these, the Simple Pile Load Test (SPLT) is developed and has applied to several construction sites so far, and proved to be efficient in terms of both time and costs(Lee et al., 1993).

In spite of its great simplicity, the method has fundamental differences from the standard conventional pile load test. These are : (1) the pile skin friction in tension instead of in compression is measured ; (2) the reduced sized core instead of the whole shoe is used for measuring the pile tip bearing capacity. Therefore, model pile load tests

¹ Associate Professor, Dept. of Civil Engineering, Korea Univ., Seoul, Korea.

² President, Piletech Co. Ltd., Seoul, Korea.

³ Researcher, The Institute of Industrial Technology, Korea Univ., Seoul, Korea.

⁴ Manager, Dohwa Soil Engineers Co. Ltd., Seoul, Korea.

using calibration chambers are performed to evaluate the effects of these differences and to recommend a reasonable prediction of ultimate bearing capacity obtained from the SPLT.

In addition, some in-situ SPLTs are performed and their results are used for modifying the Meyerhof's bearing capacity equations based on the standard penetration number.

TEST PROCEDURE OF THE SPLT

The test system is mainly composed of two parts. The first part is the separable shoe with the 'sliding core' and the second part is the loading system. Fig. 1 illustrates the separable shoe with the sliding core. The diameter of sliding core is smaller than that of the shoe. Pile load test is carried out through two successive stages. First, the shoe is inserted to the tip of the steel pipe pile, and driven into the bearing stratum through a load transferring pipe. The outside diameter of the load transferring pipe is slightly smaller than the inside diameter of the pipe pile, and is installed inside the pile with the pile top arrangement as illustrated in Fig. 2. When the load is applied to the system by the oil jack, uplift resistance is generated at the pile wall and at the same time, compressive load is transferred to the separable pile shoe through the load transferring pipe. These two forces act as the reaction forces each other until one of them reaches the failure state.

Since the shaft resistance is usually smaller than the tip resistance in most soil conditions in Korea, it reaches the ultimate state first. The pile wall movement necessary to define the ultimate and the residual shaft resistance is quite small (about 4~6 mm) and thus it does not take much time to determine the ultimate uplift capacity.

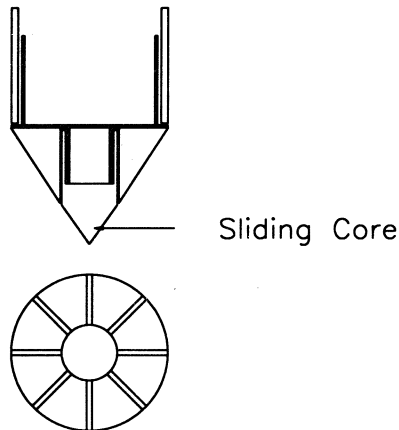


Fig. 1 Separable Shoe with Sliding Core

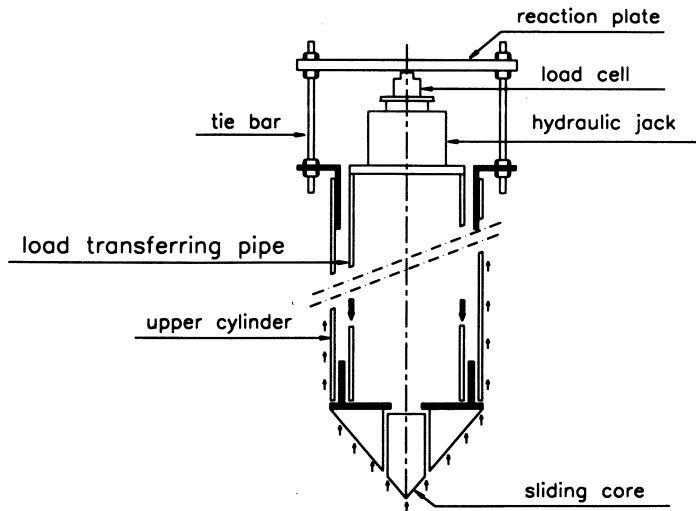


Fig. 2 First Stage of Simple Pile Load Test

Since the residual value of shaft resistance cannot resist a further increase of tip resistance, the sliding core which has a much smaller diameter than that of the whole shoe is introduced for the second stage of the test. After the determination of ultimate and residual values of shaft resistance, the pile top arrangement and load transferring steel pipe are removed. A steel rod is then attached to the lower end of the load transferring steel pipe. The diameter of the attached steel rod is slightly smaller than the inside diameter of the hole for the sliding core, so that the load is transferred directly to the sliding core (Fig. 3). As the cross-sectional area of the sliding core is much

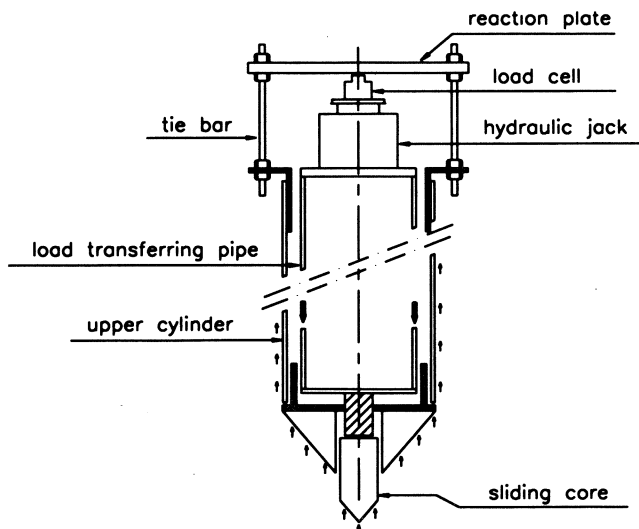


Fig. 3 Second Stage of Simple Pile Load Test

smaller than that of the whole pile tip, the increased load applied to the sliding core can now be resisted by the residual shaft resistance. By designing the appropriate dimension of the sliding core, the ultimate tip resistance can be defined. The settlement of the pile tip and the upward movement of the pile shaft are monitored via dial gages and reference beam arrangement at the pile head.

MODEL PILE TEST

Some uncertainties to be investigated through the laboratory model test are summarized into two categories: the influence of applied load direction on skin friction and the size of the pile tip on end bearing capacity. Therefore, the aims and scope of the laboratory model tests are as follows:

1. To evaluate the differences between the uplift resistance and the compressive shaft resistance, and
2. To establish a correlation between the end bearing capacity obtained from the sliding core and that of the whole pile tip.

Model Pile

To simulate the Simple Pile Load Test in a laboratory, a small-scale model pile was designed. It is desirable to make the model pile as small as possible to increase the diameter ratio (D_c/d_p : D_c = diameter of calibration chamber, d_p = diameter of penetrometer), as the larger the diameter ratio, the less the boundary effects (Parkin & Lunne, 1982). However, to accommodate the separable pile shoe with the sliding core, at least 40 mm diameter was practically required and hence 40 mm diameter steel tube with wall thickness of 1.5 mm was fabricated. Total length of the test pile without the shoe is 500 mm. The separable pile shoe with the sliding core of 14 mm diameter was attached to the pile tip. Tip angle of the shoe is 60 degrees which is almost the same as those of in-situ test piles. It is worth noted that despite the effort of minimizing scale effect, a diameter ratio, $D_c/d_p = 19$ (in this case) may cause serious boundary effects. As the boundary effect is not a major concern in this investigation, it will not be discussed in the study.

Calibration Chamber

A calibration chamber in which field stress conditions can be simulated was designed (Fig. 4). The structural parts of the chamber consist of a steel cylinder and two steel plates. The height of the chamber is 1000 mm and the internal diameter of the steel cylinder is 760 mm. A hole was drilled on the top plate for driving of the model pile. A tubular side membrane was attached to the inner surface of the steel cylinder and a flat membrane was located at the bottom plate. They serve as the lateral and the vertical pressure membranes, respectively. Pressure is independently applied to each membrane by compressed air and controlled by regulators.

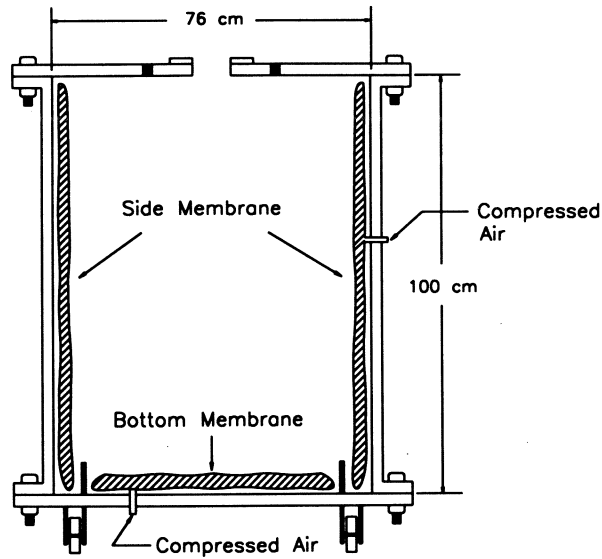


Fig. 4 Calibration Chamber

Sample Preparation

To evaluate the influence of applied load direction on skin friction and the size of pile tip on end bearing capacity, a uniform sand layer is composed. Weathered granites overlaid by sand layer is also prepared by compaction to investigate the size effect of pile tip, since most construction sites in Korea are composed of residual soils of completely weathered granite or gneiss as a bearing stratum.

Sand was deposited using the 'raining method'. In this method, streams of sand were dropped through still air at a controlled, constant height of drop to form a uniform sand deposit of a known relative density. Very high relative density (over 90%) was obtained when the free-fall height from the screen exceeds about 500 mm. Considering the total height of calibration chamber (one meter), each layer was deposited with 150 mm thickness to obtain a uniform density with depth. Tests were performed only to the dense specimen and the free-fall height was fixed at 500 mm.

Weathered granite was compacted up to 100 mm from the top of the chamber, using metal rammer weighing 75 N, sliding freely in a tube with a height of drop of 600 mm. In the upper part of the compacted granite layer, sand was deposited in the same manner of making up the uniform sand layer.

As described above, more attentions were given to stress levels than to relative densities in the test. After a specimen was prepared, vertical and lateral pressures were applied for a period. Experience showed that it takes more than 20 hours to stabilize the inside stresses (Paik et al., 1990).

Test sand was dried in air to below 2% of water content. It is a poorly graded, clean fine sand, and classified as SP by the USCS (Unified Soil Classification System). The grain size distribution is shown in Fig. 5. The maximum dry density is 16 kN/m^3 . The angle of internal friction, ϕ , of 40 degrees is obtained from direct shear test.

Weathered granitic soil was obtained in Kimcheon, Korea. Its optimum moisture content and maximum dry density are determined as 10% and 19 kN/m^3 , respectively, from laboratory compaction test. Cohesion and angle of internal friction are 30 kPa and 39 degrees at 15% strain as determined from triaxial compression test. The grain size distribution is also shown in Fig. 5.

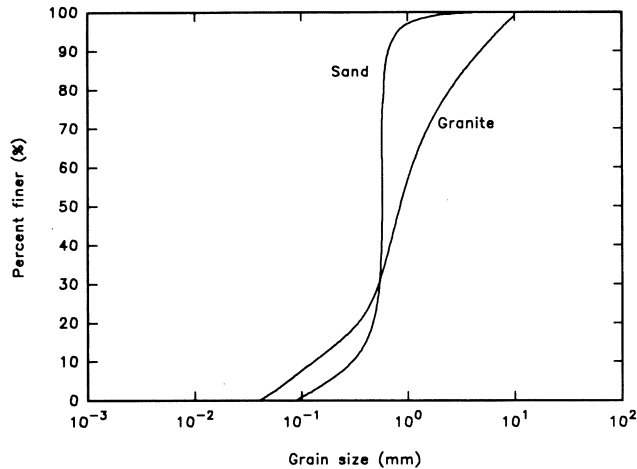


Fig. 5 Grain Size Distribution of Test Soil

Loading System and Test Procedure

Both the compressive and the tensile load are applied by oil jack which has a maximum capacity of 50 kN. Loads were measured through two proving rings of allowable capacities of 4 kN and 30 kN, respectively. The lower capacity proving ring is more sensitive and mainly used to measure the resistance in lower range, e.g., skin friction and the bearing capacity of the sliding core. Displacements were measured by two dial gauges installed at the pile head.

In the case of uniform sand layer, a series of stress conditions used are summarized in Table 1. Since the coefficient of lateral earth pressure, K_s value is reasonably assumed to be 0.4 in actual field conditions, each stress level is controlled to maintain this value.

Table 1 Stress Conditions in Laboratory Model Tests

step	1	2	3	4	5	6
σ_v (kPa)	25	50	75	100	150	200
σ_h (kPa)	10	20	30	40	60	80

In the case of granitic soil layer which simulates end bearing stratum, tests were performed in two stress conditions whose vertical components are 100 kPa and 150 kPa, and the end bearing capacity is measured.

After depositing the specimen, the top plate was positioned and it was bolted to the flange of the chamber. Both the vertical and horizontal pressures were then applied simultaneously and maintained throughout the consolidation for about one day. The model pile was then driven into the specimen using the model laboratory hammer. The hammer consists of a ram weighing 43 N, a steel guide rod running through the center hole of the ram and an anvil that fits into the head of the pile.

Schematic diagram of the test procedure is illustrated in Fig. 6. The details of pile tip behavior at each stage are illustrated in Fig. 7. Explanations of each test stage are as follow :

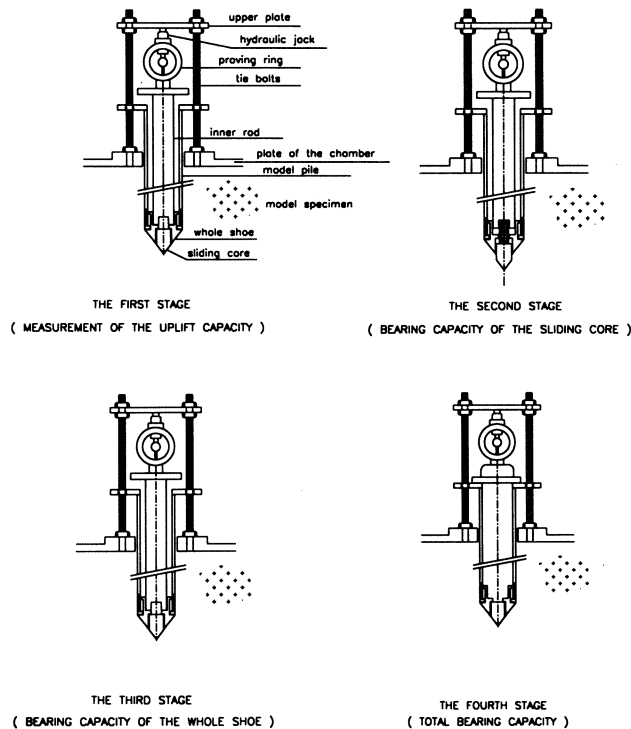


Fig. 6 Test Procedure

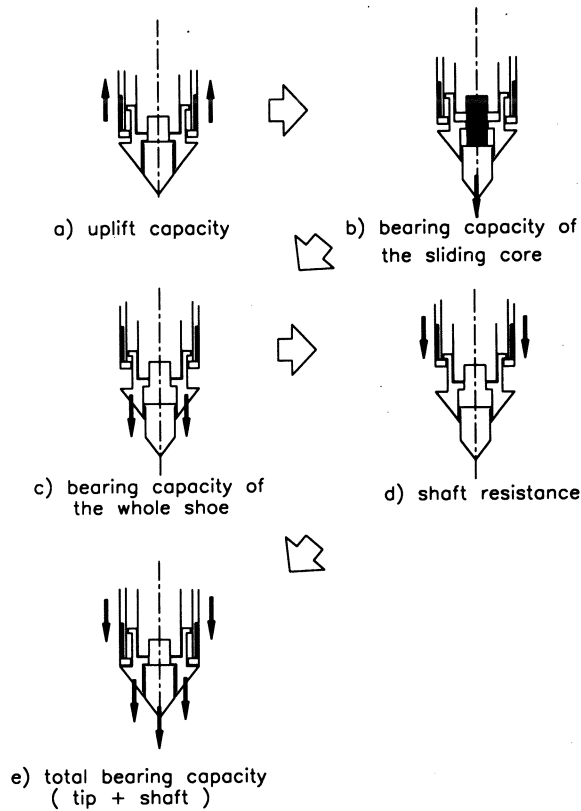


Fig. 7 Tip Behavior of Model Pile

1. First stage of the test

To measure the uplift capacity, the upper reaction plate which is exactly the same as that of the pile head is placed on the proving ring and then both plates are connected by the reaction bolts. When the oil jack begins to operate, the inner rod transfers the load to the separable pile shoe and at the same time, the model pile wall resists to the uplift load (as shown in Fig. 7a). It is almost exact simulation of the Simple Pile Load Test in the field. The uplift resistance reaches failure state prior to the pile tip in this stage.

2. Second stage of the test

After the ultimate and residual uplift resistances are determined, arrangements at the pile head are removed. The steel rod, the diameter of which is slightly smaller than that of the sliding core, is attached to the tip of the inner rod. When the inner rod is positioned, it is only supported by the sliding core. The upper reaction plate is connected to the top plate of the chamber by longer reaction bolts. Accordingly, applied

THE SIMPLE PILE LOAD TEST AND ITS APPLICATIONS

load is transferred to the sliding core and the test is performed until the sliding core settles to its maximum stroke (about 10 mm), as shown in Fig. 7b.

3. Third stage of the test

The testing procedure is the same as that of the second stage of the test, except that the steel rod is removed from the inner rod. Applied load is transferred to the whole pile tip in this stage. The ultimate bearing capacity of the whole pile tip is determined, as shown in Fig. 7c.

4. Fourth stage of the test

During the shoe settled with increase of applied load in the previous stage, it was gradually separated from the model pile itself. After the test, the shoe still remained separated from the pile. The inner rod was removed and the oil jack was directly placed on the pile head. Therefore, the applied load was transferred along the pile shaft only until the model pile reaches to the separated shoe, as shown in Fig. 7d. The shaft resistance to compressive loading is measured in this stage.

5. Fifth stage of the test

When the model pile reaches to the separated shoe, the shoe also begins to resist the external load so that both the shaft and end bearing resistance supported the applied load, as shown in Fig. 7e. Since the calibration chamber is heavy enough to provide the reaction force to the applied load, the total bearing capacity can reach the ultimate state. Tests were performed at every 50 mm depth from the embedment of 100 mm to 450 mm.

TEST RESULTS

Shaft Resistance

The ratio of uplift capacity to the shaft resistance in compression is plotted against the penetration depth in Fig. 8, resulting in the average value of 0.78. Although it is observed that the uplift capacity is smaller than the compressive shaft resistance as conventionally believed, analysis based on stress levels give somewhat different results. As shown in Fig. 9, the uplift capacity approaches to the compressive shaft resistance as stress levels increase. It means that unit shaft resistance may not change with direction of applied load as penetration depth increases in the field. In order to investigate the changes in stress conditions after pile installation, the coefficients of lateral earth pressure after pile installation, K_s , is compared with the values at rest, K_0 . The values after pile installation is larger than the values at rest as shown in Fig. 10. It indicates that in cohesionless soils, densification may occur around the pile wall even in a very dense state.

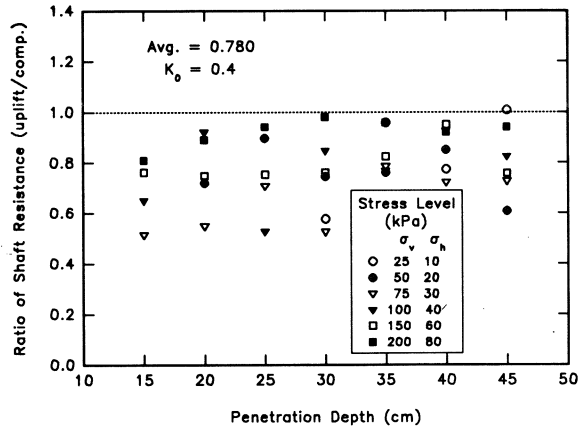


Fig. 8 Variation of Uplift/Shaft Resistance Ratio with Penetration Depth

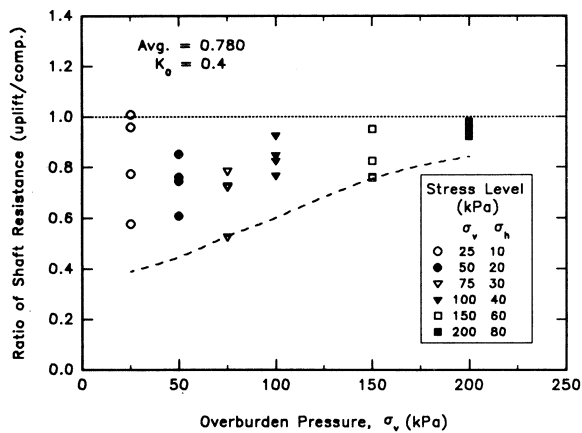


Fig. 9 Variation of Uplift/Shaft Resistance Ratio with Stress Levels

Pile Size Effect

The failure load has not been clearly defined for end bearing piles. It can be obtained from any settlement criterion which depends greatly on the pile type, diameter, length, the method of installation, and soil conditions at the site (Leonards & Lovell, 1978). In the laboratory model tests, the weight of the calibration chamber could give sufficient reaction force to both the whole pile tip and the sliding core resistance. Consequently, the end bearing capacity was viewed in terms of 'failure', that is, rapid progressive settlement at constant load.

Fig. 11 and Fig. 12 show the relationship between the end bearing capacity ratio

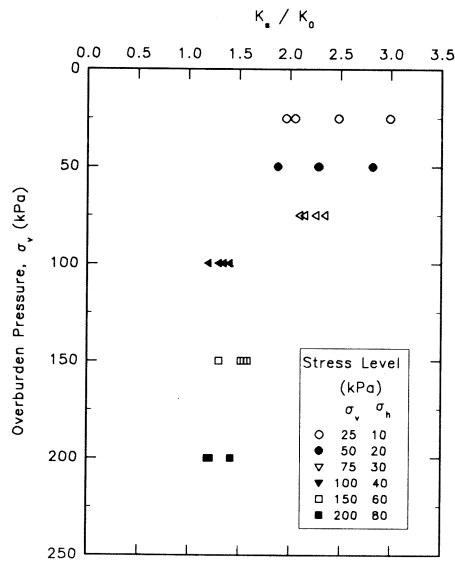


Fig. 10 Variation of Coefficient of Lateral Earth Pressure due to Pile Installation

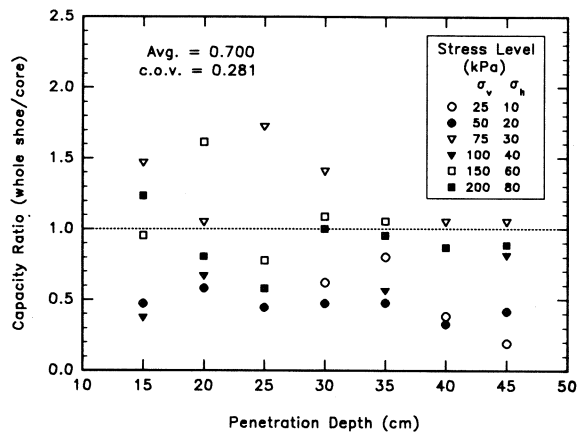


Fig. 11 Variation of End Bearing Capacity Ratio in Uniform Sand Layer

(i.e. the ratio of the whole tip to the sliding core) and the penetration depth. Fig. 11 which is the case of uniform sand layer shows the average ratio is 0.7 with the coefficient of variation of 0.281. This tendency coincides well with the explanation based on the pile size effect as already mentioned by DeBeer(1963). Fig. 12 also shows the average ratio is 1.097 with the coefficient of variation of 0.120 in the case of granitic soil layer. This result is somewhat contrary to the case of sand layer.

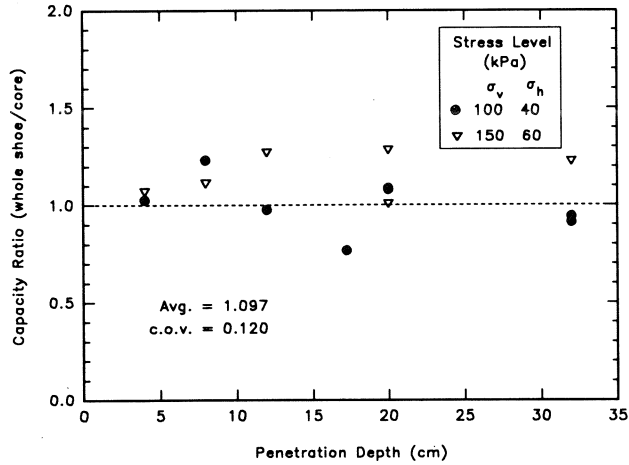


Fig. 12 Variation of End Bearing Capacity Ratio in Weathered Granites

Fig. 13 shows that the end bearing capacity becomes constant value in relatively high stress level beyond a certain penetration depth. It indicates that critical depth which means that the end bearing capacity remains constant with increase of penetration depth is 7 to 8 times to the pile diameter in uniform sand layer. Fig. 13 shows, however, that the end bearing capacity in granitic soil does not have any constant value in accordance with depth of penetration; critical depth is not observed.

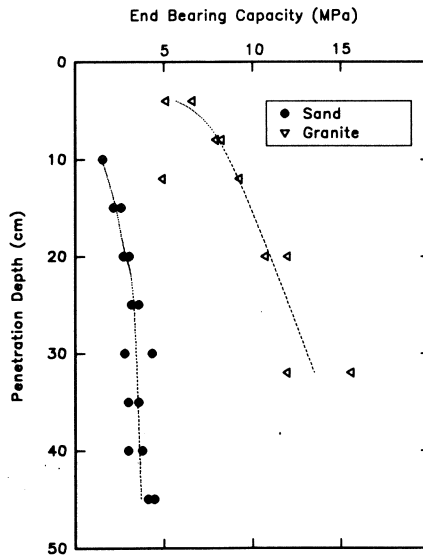


Fig. 13 Variation of End Bearing Capacity with Penetration Depth in High Stress Level

APPLICATIONS

In Korea, the formulae proposed by Meyerhof(1956) based on the standard penetration number, N-value are frequently used in the pile foundation design stage. As mentioned in the previous section the Simple Pile Load Test is able to measure the pile skin friction and the tip bearing capacity separately. In order to analyze and propose the new design correlations based on the standard penetration number, the Simple Pile Load Test have been performed at three different housing sites. One is at Changwon and the others are Sanbon and Ilsan in Korea. The geological formations of the test sites are mainly granite and gneiss whose thickness of the weathered zone varies but in most cases less than 15 m.

Skin Friction

Compacted weathered granitic soils possess both the angle of internal friction and the cohesion. However, upon saturation, the cohesion intercept becomes nil so that the material can be treated as cohesionless soils(Lumb, 1962). In most of the test locations, the ground water level is high(usually less than 2 m from the surface). It is thus possible to conclude that the skin friction is from the interaction between the pile material and the cohesionless soils

Fig. 14 shows the test results and the correlation proposed by Meyerhof, which is expressed as,

$$f_s = 2N_{sa} \quad (kPa)$$

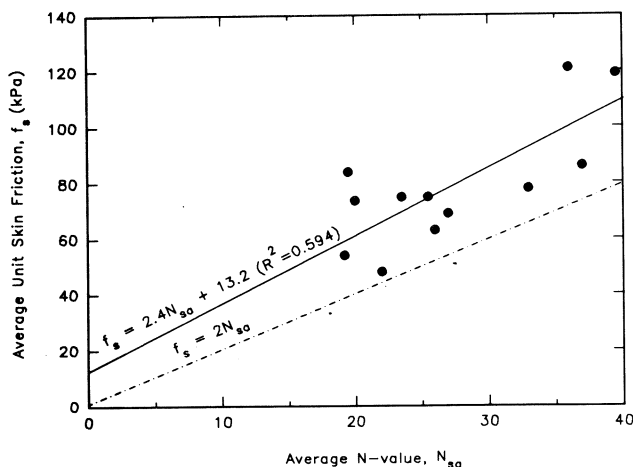


Fig. 14 Correlation of Average Unit Skin Friction with Average N-value

where f_s is unit skin friction in kPa and N_{sa} is the average N-value along the pile shaft. Fig. 14 also shows the regression line of test results of the SPLT,

$$f_s = 2.4N_{sa} + 13.2 \quad (kPa)$$

which exhibits a quite poor correlation. It is evident that the Meyerhof correlation is not applicable.

In cohesionless soil, the estimation of pile skin friction is commonly expressed as,

$$f_s = \sigma'_{va} K_s \tan \delta$$

where, f_s : unit skin friction

σ'_{va} : average vertical effective stress

K_s : coefficient of lateral earth pressure

$\tan \delta$: coefficient of friction between pile wall and soil

Using the above equation, Fig. 15 shows a new correlation of test results which is tried by plotting $K_s \tan \delta$ vs. (N_{sa}/σ'_{va}) . A much improved correlation is obtained, which is expressed as

$$K_s \tan \delta = 2.938 (N_{sa}/\sigma'_{va}) - 0.0346$$

where σ'_{va} : average vertical effective stress in kPa.

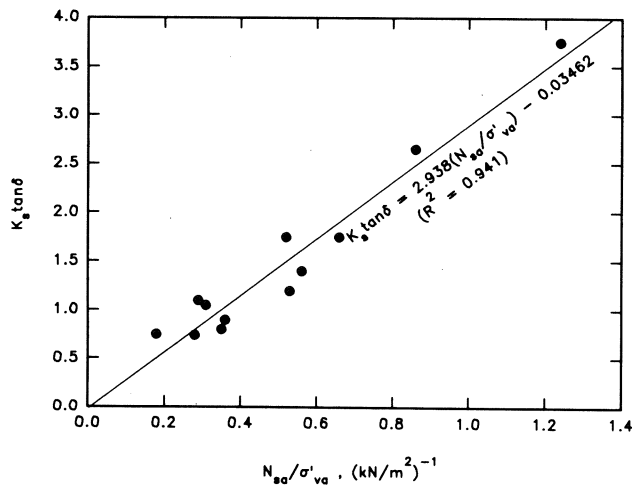


Fig. 15 (N_{sa}/σ'_{va}) vs. $K_s \tan \delta$

End Bearing Capacity

Meyerhof also proposed the correlation between end bearing capacity and N-value which is expressed as,

$$q_b = 400N_b$$

where q_b is unit end bearing capacity and N_b is average N-value near the pile end. Fig. 16 shows the ratio between the measured and the calculated using the above equation, for each of the test sites, Sanbon, Changwon, Ilsan. The figure indicates that four cases have the ratio less than 0.75 and only two cases have the ratio more than 1.0. It also shows that the above equation gives the upper bound of the end bearing capacity. Although the number of test results are not large, it is considered a reasonable conduction that the following equation is used in the design of ultimate end bearing capacity of the granitic soil stratum.

$$q_b = 300N_b$$

CONCLUSIONS

To investigate the deficiencies in the SPLT, Model pile tests were carried out using calibration chambers. The model pile test shows : 1) the uplift capacity was generally smaller than the compressive shaft resistance ; the former almost approached to the latter as the stress levels increased ; 2) critical depth as well as pile size effect was observed in the uniform sand, while it was not in the compacted granite stratum. The SPLT was applied at some construction sites in Korea using Meyerhof's bearing capacity equation based on a modified standard penetration number. The N-value was modified as appropriate to the residual soil conditions composed of granite or gneiss.

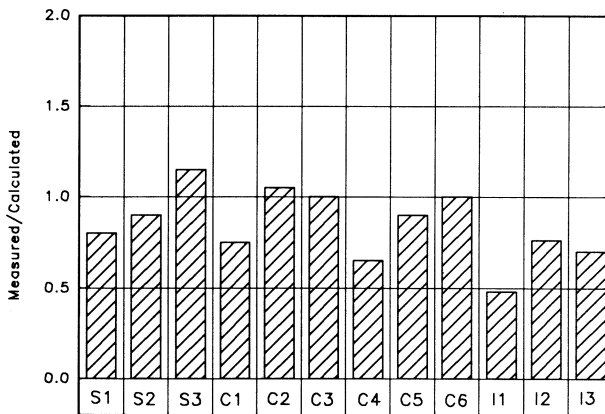


Fig. 16 End Bearing Capacity Ratio of In-situ Test

THE SIMPLE PILE LOAD TEST AND ITS APPLICATIONS

The field load test shows that Meyerhof's skin friction equation based on the standard penetration number gives a lower bound solution, and his end bearing equation gives an upper bound.

REFERENCES

- DEBEER, E. E. (1963). The scale effect in the transposition of the results of deep sounding tests on the ultimate bearing capacity of piles and caisson foundations. *Geotechnique*, Vol. 13, No. 1, pp. 39-75.
- LEE, M. W., PAIK, S. W., LEE, W. J., YI, C. T., KIM, D. Y. & YOON, S. J. (1993). The Simple Pile Load Test (SPLT). *Geotechnical Testing Journal*, Vol. 16, No. 2, pp. 198-206.
- LEONARDS, G. A. & LOVELL, D. (1978). Interpretation of load tests on high-capacity driven piles. *Symposium on Behavior of Deep Foundations*, ASTM, STP 670, pp. 388-415.
- LUMB, P. (1962). The properties of decomposed granite. *Geotechnique*, Vol. 12, pp. 226-243.
- MEYERHOF, G. G. (1956). Penetration tests and bearing capacity of cohesionless soils. *Journal of Soil Mechanics and Foundation Engineering Division*, ASCE, Vol. 82, SM 1, pp. 1-19.
- PAIK, S. W., SA, S. H., YI, C. T. & LEE, M. W. (1990). A study on the soil deformation due to a pile penetration in sandy soils. *Journal of Korean Geotechnical Society*, Vol. 8, No. 1, pp. 13-22.
- PARKIN, A. K. & LUNNE, T. (1982). Boundary effects in the laboratory calibration chamber of a cone penetrometer for sand. *NGI publication*, No. 138, pp. 307-312.

SOIL PIPE EFFECTS ON PORE PRESSURE REDISTRIBUTION IN LOW PERMEABILITY SOILS

J.J. McDonnell¹ and M.Taratoot²

SYNOPSIS

Soil structure and macroporosity greatly influence the geotechnical characteristics of natural and man-made hillslopes, including water movement and resulting slope stability. In low permeability soils, soil pipes have traditionally been identified as pathways for pore water dissipation under high rainfall and antecedent wetness conditions. A laboratory study was conducted to examine the nature of a single large pipe on pore water re-distribution and dissipation during a simulated rainstorm. Hydraulic gradients that formed during wetting remained as the system drained and steeper gradients led to slightly accelerated drainage in the vicinity of the soil pipe. Nevertheless, there was no significant difference in pore pressure dissipation between the pipes and unpiped control slope. The geotechnical implication for slope drainage in low permeability soils is that to achieve effective slope drainage from soil pipe systems, one requires an effective delivery mechanism of infiltrating rain to the pipe location before active control on pore pressure is achieved.

INTRODUCTION

Slope drainage during heavy rainfall is an important issue in civil engineering. In many areas of South East Asia, hilly terrain is prone to landslides brought about by heavy seasonal rainfall (Lumb, 1975). In other regions, several studies have been conducted to examine the role of subsurface water movement and redistribution on slope stability and landslide initiation (Neary and Swift, 1987; Sidle et al., 1985 and Sidle and Swanston, 1982).

Factors such as thin soil, steep slopes, concentrated drainage, shallow rooted vegetation and high soil clay content all promote increased susceptibility to failure (Costa, 1984). Several studies have suggested that combined with these factors one needs to understand the nature of soil piping as a geotechnical control on slope stability. In Hong Kong for example, the granites and volcanic rocks are weathered to considerable depths with surface residual soil often underlain by a mantle of colluvium. It has been shown recently that the existence of soil pipes is an important factor in the overall stability of some Hong Kong hillsides (Brand et al., 1986), and they have undoubtedly

¹ Associate Professor State University of New York

² Research Scholar, Utah State University, Logan, Utah, U.S.A., 84322

contributed to some of the failures that have occurred in Hong Kong cut slopes (Premchitt et al., 1985).

While several studies have indicated that pipes may decrease slope failure susceptibility by enhancing the effective slope drainage and pore water dissipation, Anderson et al. (1982) showed that vertical bypassing in clay shrinkage cracks in a roadway embankment resulted in faster than expected increase in pressure potential at a mid-slope soil profile. They found that water movement through seasonally active cracks led to the development of an upper zone where soil water potentials exceeded zero and produced a concomitant decrease in slope stability. McDonnell (1990) found that the presence of a well-connected pipe system at the soil-bedrock interface distributed water quickly downslope, at rates well in excess of saturated hydraulic conductivities. Under exceptionally high rainfall intensities, however, the systems of developed cracks and pipes induced slope instability by increasing the rate of infiltration over lateral pipeflow rates. This was seen to result in a build-up of pore pressure at the soil bedrock interface and subsequent slope failure. Other studies have examined the role of a single soil pipe on the geotechnical flow regime of the slope. Pierson (1983) used a Hele-Shaw (viscous flow) model to document soil pipes effects and showed that when the pipe was blocked or was a deadend passageway (a closed pipe) the cavity could be readily filled with water during a rain event, increasing pore water pressure in the surrounding matrix. Furthermore, he found that if the pipes were continuous downslope for some distance, they could generate pressure potential much greater than those generated by total saturation of the soil, enabling failure initiation at sites that would otherwise be stable. Similarly, Brand et al. (1986) documented the effect of constricted or silt-filled pipes on hillslopes in Hong Kong, that resulted in a total head increase of 4 m in 6 hrs and subsequent slope failure. The blocking-up of normally hydraulically efficient pipes was seen as the major contributing factor to frequent landsliding.

Notwithstanding the above discussion, it is clear that increased pressure potentials and soil water movement seem to be major and fundamental controls on the geotechnical integrity of slopes. While Sidle et al. (1985) have noted that little data exist on pressure potential in the soil mantle at the time of failure, some studies have suggested that near-saturation of the soil profile may be necessary to induce failure (O'Loughlin and Pearce, 1976; Pierson, 1980). Preferred flow through soil pipes greatly affects the rapidity of slope saturation, particularly under low conductivity matrix conditions. Prior studies of pipe flow contributions to subsurface stormflow (e.g., Mosley, 1979; Tanaka et al., 1988) have shown that pipes may generate subsurface flow of up to 30 m/hr via turbulent non-Darcy type flow channels.

This enhanced subsurface flow may greatly dissipated elevated pore pressures and speed slope drainage. Laboratory studies have been conducted (e.g., Anderson and Burt, 1977;

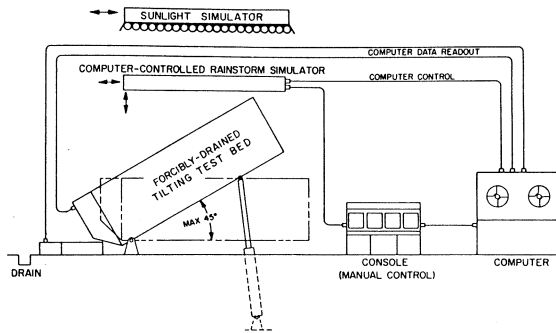
Phillips et al., 1989, Stauffer and Dracos, 1986; Kitahara et al., 1992) but have not addressed directly the issue of pipe presence on surrounding pore pressure development and dissipation. It is generally accepted that unless blocked by debris, soil pipes should

SOIL PIPE EFFECTS ON PORE PRESSURE

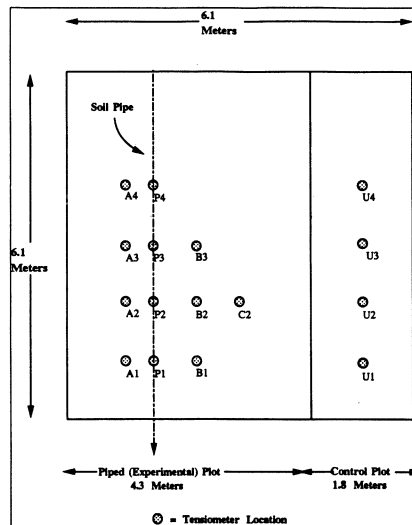
greatly assist in the dissipation of pore pressure and increase directly the rate of subsurface drainage, particularly in low permeability, two-domain soils. This study is a laboratory investigation of the effect of a single soil pipe on temporal pore pressure dissipation and spatial re-distribution of matric and pressure potentials.

METHODS

The study was performed at the Utah Water Research Laboratory and Dept. of Civil and Environmental Engineering rainfall-runoff simulator (Figure 1). The device used consists of a computer controlled rainstorm simulator, a hydraulically elevated tilting platform and soil enclosure. The 6.1 m square experimental bed was divided into two hydrologically separate hillslope plots (Figure 2). The smaller plot was 1.8 x 6.1 m and



1. The Utah Water Research Laboratory Rainfall-Runoff Simulator.



2. Experimental Plot Showing Tensiometer Locations.

was used as an unpiped control. The larger plot was 4.3 x 6.1 m and was used for the pipe experiments.

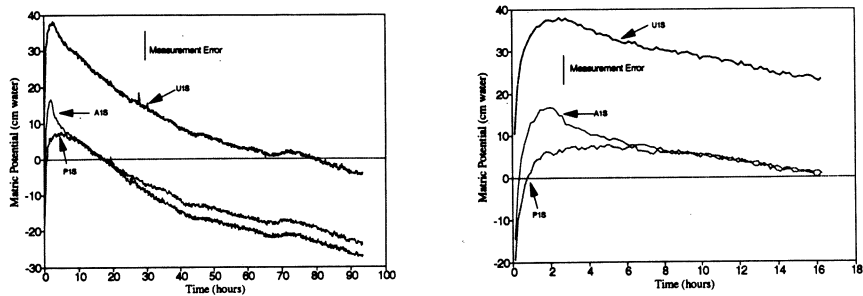
Several runs were performed. In the experiment described in this paper, rainfall was applied at an intensity of 25.4 mm/hr for 80 minutes. The bed was tilted to a slope angle of 30° and a wooden support frame was constructed at the downslope end of the bed. The support frame system acted as a seepage face; it allowed water to seep from the face while retaining the soil. The bottom 305 mm of the face was impermeable and created a “lip” that kept a small saturated wedge at the slope base.

A simulated soil pipe was installed directly above the soil base of the 4.3 m plot (Figure 2). The soil pipe consisted of a 102 mm diameter PVC leachfield pipe. Prior to installation, the pipe was perforated with hundreds of additional holes of various sizes to allow water movement into the pipe. The pipe was wrapped in a porous cloth to exclude soil. The pipe was then placed at the base of the test bed so that it extended the entire length of the slope and exited through a hole in the impermeable lip at the bottom side of the bed. The bottom end of the pipe was open to allow water to flow out into a collection bucket.

A Cache Valley loam soil was installed in the test bed to a depth of 0.65 m. The soil was 34% sand, 47% silt, and 19% clay, had a laboratory-determined saturated hydraulic conductivity of 10.8 mm/hr and a bulk density of 1.1 g/cc. A recording tensiometer network was installed, similar to that described in McDonnell (1993). The system consisted of 32 Soilmoisture Equipment Corp. manometer cup tube kits connected via a fluid line to 32 SenSym Inc. SCX15DN temperature-compensated differential pressure transducers. The transducers were all located at a common elevation (datum). The millivolt output from the transducer was recorded at 10 minute intervals using a Campbell Scientific Inc. CR10 micrologger and AM416 multiplexer. Precision of the tensiometer-transducer system was +/-5 cm H₂O.

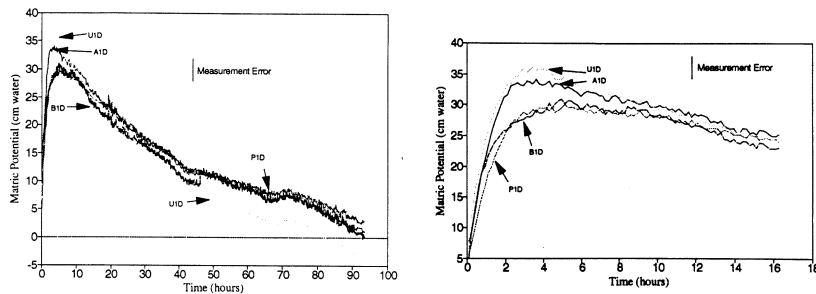
RESULTS

Figure 3a shows the time series response of soil water potential to the rainfall



3. Soil Water Potential Indicated by Shallow Tensiometers 1 m Upslope for the (a) complete wetting and drying cycle and (b) in detail for the first 18 hours of wetting (80 min) and subsequent drainage.

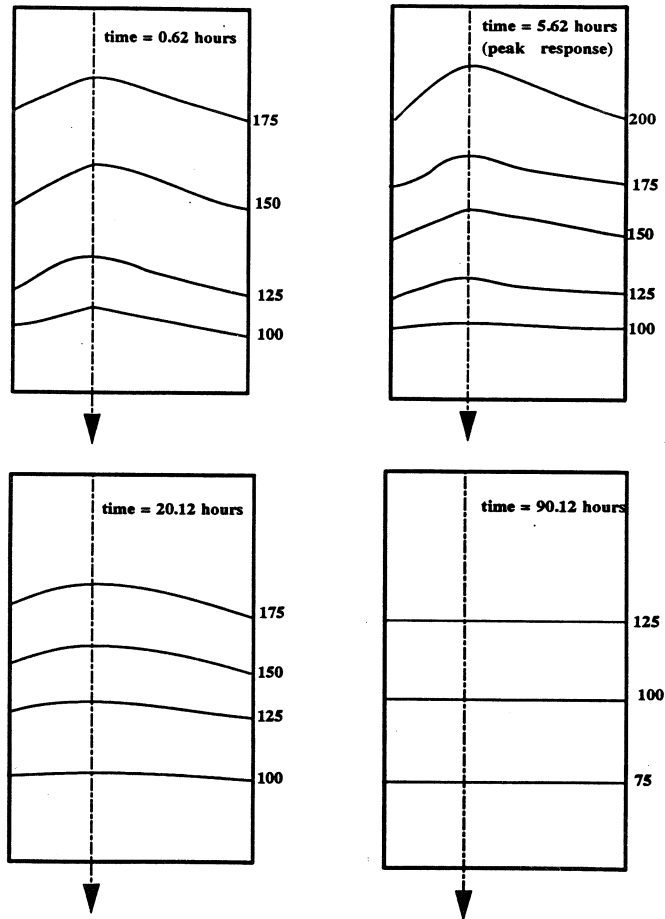
application 1.0 m upslope for the shallow (0.15 m) tensiometers A, P and U. Figure 3b shows only the first 18 hours of the experiment. Sensor B failed and is not shown on the graphs. The plots indicate saturation across the plot. The peak pore pressure (pressure potential) on the control plot with no pipe is 38 cm H₂O. The peak pore pressure on the plot with the pipe is only 8 cm H₂O over the pipe and 17 cm H₂O at a horizontal distance 0.5 m from the pipe. This indicates that at shallow depths, there is pipe control on total pore pressure, with more subdued peak response over the pipe and sharper shifts in pressure at locations away from the pipe. After peak response, nevertheless, recession of pore pressure from all three sensors was at the same rate. Figure 4a shows the time series of pressure and matric potential response (positive and negative pore pressure, respectively) for all the deep (0.45 m) sensors 1.0 m upslope from the downslope end of the testbed.



4. Soil Water Potential Indicated by the Deep Tensiometers 1 m Upslope for the (a) complete wetting and drying cycle and (b) in detail for the first 18 hours of wetting (80 min) and subsequent drainage.

Figure 4a shows the first 18 hours of response in greater detail. Peak response is greater on the control plot than on the piped slope, but the difference in peak pressure potential is less than in Figures 3a and b. Peak response on the control plot is 36 cm H₂O. Directly over the pipe, peak response is 30 cm H₂O. The difference in peak response between the piped and unpiped plot is within experimental error. Recession appears to start sooner at locations over the pipe and 1.0 m away from the pipe than at 0.5 m away from the pipe on the control slope. During recession, the matric potential declines more quickly on the control plot. After 24 hours, the matric potential on the control plot is more negative than at any location on the piped plot at the same distance upslope. However, the difference always remains within experimental error.

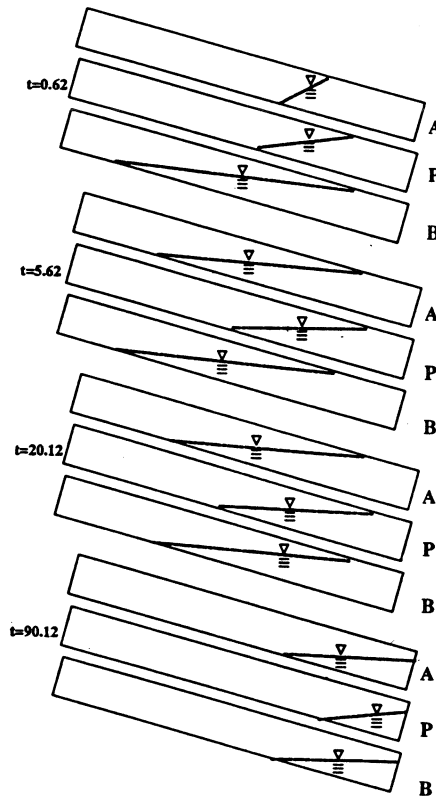
A selected series of plan view diagrams of total water potential is shown in Figure 5. There is evidence that flow converges toward the pipe throughout the experiment, indicating that the pipe may influence the spatial redistribution of pore pressure on the slope. After 90 hours, flow appears to be uniform in the downslope direction, with no sign of convergence toward the pipe.



5. Plan-View Isopotential Diagrams for Selected Times through the Experiment.

Figure 6 shows the shape and upslope extent of the water table for selected times through the experiment. Positions P, A, and B are directly over the pipe, 0.5 m, and 1.0 m from the pipe respectively. These diagrams show only the bottom 4 m of the experimental hillslope. During the experiment the water table expands upslope and then dissipates during drainage. At maximum response, the water table moves farther upslope at locations away from the pipe. As one would expect, the water table dissipates more quickly over the pipe; in reality, however, this difference in dissipation is only marginal. While the geometry of the water table is different, water table longevity is essentially the same between slope profiles.

SOIL PIPE EFFECTS ON PORE PRESSURE



6. Cross-Sectional Watertable Diagrams for Selected times through the Experiment, where: A, P and B represent different tensiometer transects upslope.

GEOTECHNICAL IMPLICATIONS

In low permeability soils, large soil pipes may not effectively contribute to rapid dissipation of elevated pore pressures. Unlike earlier studies by McDonnell (1990), this study shows that while the soil pipe had some effect on spatial redistribution of pore pressure during drainage, peak pore pressure response and dissipation was not significantly different between the a piped slope profile and the unpiped control slope profile. Obviously, natural soil pipes are much more complex entities than the laboratory soil pipe described here. The present study represents an idealized condition with straight, uniform pipes. Notwithstanding, for rapid discharge or soil water potential dissipation by soil pipes, it appears that additional factors may be required or need to be met for effective pore pressure dissipation. For instance, Anderson et al. (1982) found that vertical bypassing was an important element in embankment stability in Hong Kong, due primarily to rapid infiltration and translocation of the water input. Similarly,

McDonnell (1990) found that a well-connected system of vertical cracks feeding the subsurface pipe system was critical to pipe control of slope drainage and elevated pore pressure dissipation. In the present study, matrix saturated hydraulic conductivities were <11 mm/hr and soil was repacked resulting in an absence of any vertical cracking or other forms of secondary porosity. As a result, the large pipe was ineffective in significantly reducing pore pressure build-up. Under natural and engineered hillslopes, it appears that the opportunity to feed water to the soil pipe system is central to its function as a slope stabilizer in low permeability soils. This study is representative of upslope areas where a pipe is collecting water. Caution should be taken in applying the results to the situations which are greatly different from the model configuration.

REFERENCES

- ANDERSON, M.G. & T.P BURT (1977). Laboratory model to investigate the soil moisture conditions on a draining slope. *Journal of Hydrology*, vol. 33:383-390.
- ANDERSON, M.G., HUBBARD, M. & KNEALE, P.E. (1982). The influence of shrinkage cracks on pore-water pressures within a clay embankment. *Quarterly Journal of Engineering Geology*, vol. 15, pp 9-14.
- BARCELLO, M. D. and NIEBER, J.L. (1981). Simulation of the hydrology of natural pipes in a soil profile. *American Society of Agricultural Engineers Paper 81-2028*. St. Joseph, Michigan. Presented at ASAE 1981 Summer Meeting.
- BRAND, E.W., DALE, M.J. & NASH, J.M. (1986). Soil pipes and slope stability in Hong Kong. *Quarterly Journal of Engineering Geology*, vol. 19, pp 301-303.
- COSTA, J.E. (1984). Physical geomorphology of debris flows. In: Costa, J.E. and Fleisher, P.J. (eds), *Developments and Applications of Geomorphology*, Springer, Berlin, pp 268-313.
- KITIHARA, H., SIDLE, R. C., TERAJIMA, T. & NAKAI, Y. (1992). Hydraulic experiments of saturated throughflow with an artificial soil pipe. In: *Transactions of 103rd Annual Meeting of Japanese Forestry Society*. Tokyo, Japan, pp. 589-591.
- LUMB, T. (1975). Slope failures in Hong Kong. *Quarterly Journal of Engineering Geology*, vol. 8, pp 31-65.
- MCDONNELL, J. J. (1990). A rationale for old water discharge through macropores in a steep, humid catchment. *Water Resources Research*. vol. 26, pp 2821-2832.
- MCDONNELL, J. J. (1993). Electronic versus fluid multiplexing in recording tensiometer systems. *Trans. American Society of Agricultural Engineers*, vol. 36, pp 459-462.
- MOSLEY, M.P. (1979). Streamflow generation in a forested watershed, New Zealand. *Water Resources Research*, vol. 15, pp 795-806.
- NEARY, D.G. & SWIFT, L.W. (1987). Rainfall thresholds for triggering a debris

SOIL PIPE EFFECTS ON PORE PRESSURE

- avalanching event in the southern Appalachian Mountains. *Reviews in Engineering Geology*, vol. 14, pp 41-46.
- O'LOUGHLIN, C.L. & PEARCE A.J. (1976). Influence of Cenozoic geology on mass movement and sediment yields in small forest catchments, North Westland, New Zealand. *Bulletin of the International Association of Engineering Geology*, vol. 14, pp 41-46.
- PHILLIPS, R.E., QUISENBERRY, V.L., ZELENIK, J.M. & DUNN, G.H. (1989). Mechanism of water entry into simulated macropores. *Soil Science Society of America Journal*, vol. 53, 1629-1633
- PIERSON, T.C. (1983). Soil pipes and slope stability. *Quarterly Journal of Engineering Geology*, vol. 16, pp 1-11.
- PREMCHITT, J., BRAND, E.W. & PHILLIPSON, H.B. (1985). Landslides caused by rapid groundwater changes. *Proc. of the 21st Regional Conference of the Engineering Group of the Geological Society of London, Sheffield*, pp 31-42.
- SIDLE, R.C., PEARCE, A.J. & O'LOUGHLIN (1985). Hillslope stability and landuse. *Water Resources Monograph 11*, American Geophysical Union.
- SIDLE, R.C. & SWANSTON, D.N. (1982). Analysis of a mall debris slide in coastal Alaska. *Canadian Geotechnical Journal*, vol. 19, pp 167-174.
- STAUFFER, F. S. & DRACOS, T. (1986). Experimental and numerical study of water and solute infiltration in layered porus media. *Journal of Hydrology*,. vol. 84, pp 9-34.
- TANAKA, T., YASUHARA, M. & MARUI, A. (1988). The Hachioji Experimental Basin Study — Storm runoff processes and the mechanism of its generation. *Journal of Hydrology*, vol. 102, pp 139-164.

Closure to Discussion on “Hyperbolic Method for Evaluation of Settlement of Ground Pretreated by Drains and Surcharge”¹

by Dr Tan Siew Ann, Dept of Civil Engineering, National University of Singapore, 10 Kent Ridge Crescent, Singapore 0511.

The author would like to thank the discussers' for their interest in the paper and their comprehensive list of papers on applications of the hyperbolic technique in predicting ultimate settlements based on their experiences in PWD, Singapore. Subsequent to the above paper, the author has published another paper (Tan 1995), to clearly set out the theoretical basis for the hyperbolic method in ultimate settlement prediction. In this recent work, the author established that the linear portion of the hyperbolic plot of t/δ vs t in theory, exist between the 60% and 90% settlement points with r^2 coefficients better than 0.999, rather than the 50% and 90% points where r^2 coefficients are only better than 0.995. This is in agreement with the work of Sridharan et al, 1987, who showed that the rectangular hyperbola for Terzaghi consolidation settlement plot is highly linear between the 60% and 95% consolidation stages.

What needs to be pointed out is that for the case of vertical drains, the ultimate primary settlement is not simply the inverse slope of the first linear portion. The simple inverse slope method would clearly over-estimate the ultimate primary settlement by as much as 20% in some cases, as shown by Tan (1995). The correct observation for vertical drains based on the theoretical plots of T/U vs T is that the slopes (α) of the first linear portions are functions of soil and drain parameters. The basis of the hyperbolic method then is shown in Fig. 1. When settlement data is plotted in the form of t/δ vs t , the ratio of slopes between the field plot and theoretical plot by comparison of the two as in Fig. 1, can be defined by:

$$\frac{S_{60}}{S_i} = \frac{\alpha_{60}}{\alpha} \quad \text{ie} \quad S_{60} = (1/0.6) \left(\frac{S_i}{\alpha} \right) \quad (1)$$

$$\text{Similarly} \quad S_{90} = (1/0.9) \left(\frac{S_i}{\alpha} \right) \quad (2)$$

By constructing these radiating lines to intersect the first linear portion of the field, hyperbolic plot, the 60% and 90% settlement points can be located, from which the ultimate primary settlement can be estimated as $(\delta_{60/0.6})$ or $(\delta_{90/0.9})$. Based on Eq.(1), the radiating line to the 60% settlement point in the field hyperbolic plot, can also be expressed as:

$$(t/\delta) = (1/0.6) (S_i/\delta)t \quad (3)$$

¹ June, 1994, Vol. 25, No. 1, pp. 75-90 by S.A. Tan

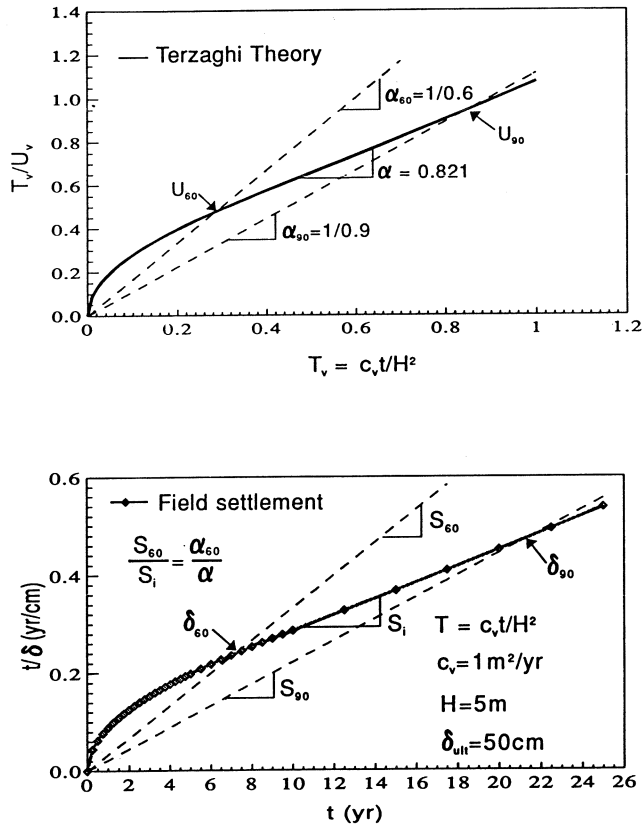


Fig. 1. Tan, S.A. Comparison of Terzaghi and Field Hyperbolic Plots.

At the intersection of this radiating line with the first linear portion of the field hyperbolic plot, t_{60} is the time and δ_{60} is the settlement at 60% consolidation. Thus, δ_{60} can also be obtained from Eq.(3) at $t_{60}/(t_{60}/\delta_{60})$, which is (0.6) (α/S_i) . Thus the ultimate settlement which is $(\delta_{60}/0.6)$, can also be computed by (α/S_i) . Based on theory, the ultimate primary settlement can be obtained from any of the three expressions:

$$\delta_{60}/0.6 = \delta_{90}/0.9 = \alpha/S_i \quad (4)$$

The writers are correct in their observations that the new method are variations of the inverse slope approach. However, the proposed method allow for the check of estimates by three different computations which should all agree if the settlement is indeed linear in the hyperbolic plot. This would serve as a simple and yet effective means to the gauge the correctness of the estimation of ultimate settlements by the

hyperbolic fitting methods for determining the degree of consolidation using vertical drains in field projects.

REFERENCES

- SRIDHARAN, A., MURTHY, N.S., and PRAKASH, K. (1987), "Rectangular hyperbola method of consolidation analysis," *Geotechnique*, Vol. 37, No. 3, pp 335-368.
- TAN, S.A. (1995), "Validation of hyperbolic method for settlement in clays with vertical drains," *Soils and Foundations*, Vol. 35, No. 1, pp 101-113.

Book Review

Book Title: **Displacement Based Aseismic Design Charts for Rigid Walls** by Dr. Shamsheer Prakash, Professor of Civil Engineering, University of Missouri - Rolla, Y. Wu and E. Arni Rafnsson.

Book description: In this manual, charts have been prepared to compute displacements for walls due to sliding and rocking under earthquakes. The walls considered are 4m - 10m high, ground motion of 0.1g - 0.5g, earthquake magnitudes of M5.25 - M8.5 and seven different types of base soils and three backfills with 3675 possible combinations. The wall sections have been designed for static factors of safety against sliding, rotation and bearing capacity first. Then their displacements were computed with *non-linear base soil as well as non-linear backfill*.

Design charts have been prepared for displacements of 5% and 10% of the height of the wall. This is the first "*displacement based design manual*" developed for use by the practicing engineers. The price is US\$30.00 including shipping by air mail.

Errata on

Discussion Paper on “Hyperbolic Method for Evaluation of Settlement of Ground Pretreated by Drains and Surcharge” by S.B. Tan and T.K. Lim, Geotechnical Engineering, Vol. 26, No. 1, June, 1995.

Re: Misprints of Initials and Omission of a Reference Title

The initials, “**T.L. Lim**”, have been misprinted as “**T.K. Lim**”.

In addition, the following reference title has been omitted from the list of references:

TAN S.B. et. al. (1985). “Soil Improvement Methods in Singapore”. Proc. 3rd Int. Geot. Sem. on Soil Improvement Methods, Singapore, pp. 249-271.

It's easy to say that your drain is better than Colbondrain® It's harder to prove it!



Colbondrain - prefabricated vertical drain - is produced and marketed by Akzo Nobel Geo-synthetics in the Netherlands and, unlike some other manu-

facturers we don't make claims that will stretch your imagination! Over one hundred million metres have been supplied worldwide, in the last twenty years for a wide range of construction projects. As you would expect, Colbondrain's quality assurance is backed by the

award of an ISO 9001 Certificate and the resources of one of the largest chemical companies in the world. Because of our unique 3D filament core struc-

ture, all the space within Colbondrain is fully inter-connected for maximum efficiency of water discharge. Even if Colbondrain is buckled by settlements, this high discharge rate will not be affected.

Ask these clients about their experience with Colbondrain:

•**Tseung Kwan O Industrial Estate**, Hong Kong, 5.3 million linear metres for Territories Development Dept, Govt of Hong Kong. •**North Lantau Expressway**, Hong Kong, 8.3 million linear metres for Highways Dept, Govt of Hong Kong. •**Bangkok Outer Ring Road**, Bangkok Chonburi Highway, Thailand, 12.0 million linear metres for Department of Highways, Govt of Thailand. •**Changi 3rd Runway**, Singapore, 19.0 million linear metres for P.S.A., Govt of the Republic of Singapore.

Colbondrain from Akzo Nobel, quality and efficiency that we can prove!

Akzo Nobel Geosynthetics, Postal address c/o Akzo Nobel Chemicals Pte Ltd,
510 Thomson Road, #15-01/02 SLF Building, Singapore 298135,
Tel. (65) 25 81 333, Telex RS 23350, Fax (65) 25 98 607.

Akzo Nobel Geosynthetics also supplies Enkadrain®, Fortrac®, Armater®, all materials are produced and supplied in accordance with the ISO 9001 quality assurance standard. (Certificate No. 935136) (*reg. trademark)

NOTES FOR THE GUIDANCE OF AUTHORS

General: Manuscripts of original papers, technical notes and discussions should be submitted to the Editor, Geotechnical Engineering, Planning Division, Civil Engineering Department, 101 Princess Margaret Road, Homantin, Kowloon, Hong Kong. Papers will be accepted for review on the understanding that they have not been submitted or published elsewhere and that they become the copyright of the South East Asian Geotechnical Society.

Papers on major geotechnical topics of wide interest to the South East Asian region are welcomed, whereas those of a specialist interest that are more suitable for other specialist journals are less likely to be accepted. Normally, papers should not exceed 16 pages, including references, figures and tables: there are about 450 words on a printed page. Short topical papers of 8 pages or less will be reviewed more quickly.

The format which must be followed for the preparation of manuscripts is in general that adopted in this issue of the Journal. Manuscripts which do not conform to this format will be returned to the author(s) without review.

Three complete copies of the manuscript, in English, should be submitted to the Editor (two copies for technical notes and discussions) together with the original drawings and photographs. In addition, a copy of the text should be submitted on 5 1/4" or 3 1/2" floppy disc formatted using DOS 3.0 (or later version) and the file should be in ASCII or Wordperfect 5.0 (or later version) format. Typescripts must be accurate and in their final format as outlined below. Owing to the high cost of corrections at proof stage, the Editor reserves the right to charge authors the full cost of corrections resulting from changes made at the proof stage.

Layout: Typescripts must be double spaced, including references, on one side only of A4 paper, with a 25 mm margin on each side. All pages should bear the authors name and be numbered serially. Papers should be succinct and arranged as follows:

1. **Title:** brief and specific in bold and uppercase, centred at the top of the first page
2. **The author(s) full name(s) should appear centred below the title in bold.** The author(s) position and affiliation should be indicated as a footnote at the bottom of the first page. A synopsis (with main heading) of not more than 200 words should appear immediately below the authors name(s). The synopsis must be intelligible without reference to the paper and should highlight the essential new information and interpretations in the paper; it should not be a mere recital of the subjects covered. A synopsis is not required for technical notes.
3. **Figures** should be drawn boldly in black ink on one side of good quality tracing paper or smooth white board, with a line weight and lettering suitable for reduction to fit the journal page width. A separate caption list should be included. All maps should include a metric scale and north point. **Photographs** should be sharp and of good contrast (black and white preferred). The authors name should be given on each sheet and the "top" indicated.
4. **Formulae** should be expressed as simply as possible, and lengthy proofs avoided. **SI units** should be used throughout.
5. **Symbols** should be defined when they first appear.
6. **References** should appear in the text as the author(s) name(s) followed by the year of publication in brackets. A list of references should be given at the end of the text in alphabetical order of author(s) name(s) with the author(s) name(s) in capitals and bold. Some examples of the format to be used in the reference list are given below:

PREMCHITT, J. & SHAW, R. (1991). Marine geotechnical engineering for development projects in Hong Kong. *Proceedings of the International Workshop on Technology for Hong Kong's Infrastructure Development*, Hong Kong, pp 721-738.

PUN, W.K. (1990). Seismicity of Hong Kong. M.Sc. Thesis of the University of London (unpublished)

PUN, W.K. & AMBRASEYS, N.N. (1992). Earthquake data review and seismic hazard analysis for the Hong Kong region. *Earthquake Engineering and Structural Dynamics*, vol. 21, pp 433-443.

HOEK, E. & BROWN, E.T. (1982). *Underground Excavations in Rock (2nd Edition)*. The Institution of Mining & Metallurgy, London, 527 p.

GEOTECHNICAL ENGINEERING

CONTENTS

Photographic Feature:

PVD Ground Improvement of Soft Bangkok Clay by Y. TAESIRI and D.T. BERGADO	1
---	---

Main Papers:

Statistical Modelling of Randomly Distributed Fibre-Reinforced Sand by G. RANJAN, R.M. VASAN and H.D. CHARAN	3
Cation Exchange Studies on a Lime Treated Marine Clay by G. RAJASEKARAN and S. NARASIMHA RAO	19
The Simple Pile Load Tests and Its Application by I.M. LEE, M.W. LEE, J.H. LEE and S.W. PAIK	37
Soil Pipe Effects on Pore Pressure Redistribution in Low Permeability Soils by J.J. MCDONNELL and M. TARATOOT	53

Closure Discussion:

Hyperbolic Method for Evaluation of Settlement of Ground Pretreated by Drains and Surcharge by S.A. TAN	63
Book Review	67
Errata	69
Advertisement	71

Abstracted and/or Indexed in *Geotechnical Abstracts*